Construction and Building Materials 411 (2024) 134441

Contents lists available at ScienceDirect

Construction and Building Materials

journal homepage: www.elsevier.com/locate/conbuildmat

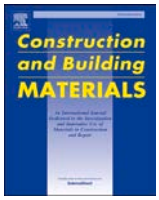

Living in the shadow of Vesuvius: Analysis of the wall paintings of Pollena Trocchia's Roman buildings across historical eruptions

Sabrina Pagano [a,b], Chiara Germinario [b,*], Alberto De Bonis [c,d], Mariano Mercurio [b,c], Girolamo Ferdinando De Simone [e], Rebecca Piovesan [f], Francesca d'Aniello [d], Celestino Grifa [b,c]

[a] Department of Science of Antiquities, Sapienza University of Rome, Piazzale Aldo Moro 5, 00185 Rome, Italy
[b] Department of Science and Technology, University of Sannio, 82100 Benevento, Italy
[c] CRACS, Center for Research on Archaeometry and Conservation Science, Via Cintia 21, 80126 Naples, Italy
[d] Department of Earth Sciences, Environment and Resources, University of Naples Federico II, Via Cinthia, Naples, 80126 Naples, Italy
[e] Università degli Studi Suor Orsola Benincasa, Via S. Caterina da Siena, 37, 80132 Naples, Italy
[f] LAMA - Laboratory for the Analysis of Ancient Materials, University Iuav of Venice, Calle della Laca, San Polo 2468, 30125 Venice, Italy

ARTICLE INFO

Keywords:
Roman wall painting
Multilayer plasters
Pigments
79 CE eruption
Archaeometric analyses
Vesuvius environs

ABSTRACT

Through a multi-analytical approach the research focused on the evolution of wall painting technology used for two decorated buildings in *Pollena Trocchia* buried by volcanic deposits of Vesuvius. The study highlighted a different stratigraphy (with two or three layers) of mortar-based supports. Volcanic aggregate was added to lime binder for *rinzaffo* and *arriccio*, whereas calcite and marble dust first, then organogenic limestones were used for *intonachino*. Pictorial layers, applied using fresco and mezzo-fresco techniques, were obtained combining common (e.g., ochre) and expensive pigments (e.g., cinnabar, aragonite, Egyptian blue), showing diachronic changes in raw materials selection and the refinement of decoration.

1. Introduction

The decorations that adorned the rooms of private *domus*, villas, and public edifices are the primary form of pictorial art linked to the ancient Roman world [1]. Formerly, this form of art was object of study by archaeologists and art-historians who were able to describe, besides the artistic values of wall paintings, the evolution of styles even in their chronological framework. In the meanwhile, over the last years, the material culture and techniques employed for wall paintings have become the subject of growing interest in different academic fields, stimulating interdisciplinary research between humanities and sciences. These researches focused on the study of pigments, their availability and provenance as well as the methods and materials used for preparing the supports to the pictorial layers [2–6]. In fact, the wall paintings need to be intended as a stratigraphy with skilled implementation of natural materials, binders and aggregates for plasters, pigment and mediums for pictorial layers, which reveal the painter's ability beyond the artistic accomplishments [7–12].

The environs of Vesuvius are an exceptional context to highlight these facets due to several reasons; above all, the state of conservation of artefacts and buildings sealed by the products of Somma-Vesuvius eruptions that also gave the opportunity to have a precise chronology of the events. In this part of the Campania region, archaeological sites are exemplary evidence for the study of the wall painting technique [13–15] that qualifies the function of the building in private and public contexts. These sites deeply influenced the studies of Roman painting to such an extent that art historians identified the so-called 'Pompeian styles' [16], which define specific artistic choices and chronological phases.

By using a multi-analytical approach consisting of non-destructive and micro-destructive techniques, the research of the recent years has brought to light many of the construction and pictorial features employed by the ancient Roman masters [4,12–14,17]. Notably, both natural and artificial aggregates were utilised according their specific properties (e.g., marble dust employed to ensure specific waterproofing characteristics) [18]. It is worth to note that a significant portion of research endeavours on this subject is focused on the Pompeian archaeological context [18–22]. This focus is attributed to the unique and exceptional nature of this context, which allows for a comprehensive archaeometric characterization of painted plasters. However, Vesuvius' environs are not only *Pompeii* or *Herculaneum*; the witnesses of the Roman artists can be also found in isolated contexts, and the

* Corresponding author.
E-mail address: chiara.germinario@unisannio.it (C. Germinario).

https://doi.org/10.1016/j.conbuildmat.2023.134441
Received 7 August 2023; Received in revised form 29 November 2023; Accepted 3 December 2023
Available online 20 December 2023

archaeological site of *Masseria de Carolis* in *Pollena Trocchia* is an example [23–25]. The site, located on the northern slopes of Somma-Vesuvius volcano, had several, subsequent lives, marked by the 79 and 472 CE eruptions until the Late Antiquity eruption cycle (505–512 CE). Firstly, beneath the pyroclasts of 79 CE (Pompeii) eruption, archaeologists discovered the remains of an ancient Roman *villa* dated back to at least the 1st century CE. Later, above the 79 CE products, a *villa* with baths was constructed and then buried by the pyroclasts of the 472 CE (*Pollena*) eruption. The discovery, awarded with the prestigious Heritage Prize 2011 from the European Association of Archaeologists, was revolutionary and enriched the knowledge about the history of the Vesuvian environs, as a testimony, along with other scatter examples [26,27], of a former reoccupation of the (northern) Vesuvian area after the 79 CE eruption.

In the examined site of *Masseria de Carolis*, the archaeological layers before and after the 79 CE eruption gave back decorated plasters still maintaining their vivid colours [24]. Although it is a fragmentary repertoire, the fragments represent a valuable opportunity to study wall painting materials and to evaluate the diachronic evolution of wall painters' techniques. These findings expand our understanding of ancient Roman construction techniques and provide valuable insights into their material choices and technological innovations, contributing to a broader comprehension of this historical period.

2. Archaeological site and materials

The archaeological site of *Masseria De Carolis*, located in *Pollena Trocchia*, a small town close to Naples (Campania region), lied on a natural slope, near the east-west axis that once connected the coastal area of *Herculaneum* with the territory of *Nola* [23] (Fig. 1a).

In 1988, the archaeological site was accidentally discovered during the dig of the volcaniclastic deposits for building purposes, and it was initially interpreted as a large warehouse for agricultural products of the 2nd century CE, buried by the 472 CE eruption. However, within two decades from the discovery, the masonry structures were covered by illegally dumped wastes. Only in 2004 the site was resumed within the interdisciplinary research called "*Apolline* Project" focused on the study of the ancient territories of *Neapolis* and *Nola*, considered as representative inhabited settlements of the northern slope of Somma-Vesuvius [24].

The site preserved a significant portion of the original stratigraphy, facilitating the development of a chronological framework that delineated the distinct phases of occupation linked to the Somma - Vesuvius eruptions. The 79 CE Pompeii eruption sealed the remnants of a *villa* decorated with wall paintings that report to decoration related to the transition between the third and fourth Pompeian styles [28].

After the Pompeii eruption, a new building dated at the end of the 1st/beginning of the 2nd century CE, was directly founded on 79 CE ash deposits [23,25]. The building included approximately 20 rooms of a *villa* with baths that extended beyond the eastern boundary [29] (Fig. 1b). Most of such structures showed evidence of their original vaulted roofs, while the occurrence of collapsed walls suggested the presence of a second floor. The discovery of fragmented mammary tiles, mosaic tiles, glass artefacts, along with remnants of wall paintings and architectural stuccos, provides evidence of the opulence of the building [24].

The *villa* was in use for at least two centuries; the northern area partially collapsed likely after an earthquake, whereas the rest of the building was in use up to the 472 CE *Pollena* eruption, which buried the structures providing an *ante quem* reference point.

Finally, another occupation after 472 CE occurred as the archaeological evidence suggested, up to the events of Late Antiquity eruption cycle (505–512 CE), when a dense layer of ash definitely buried the site [23].

To define the wall painting techniques used in the Roman settlements of *Pollena Trocchia*, the multi-analytical study was carried out on eight samples of decorated plasters. The study centred on fragments excavated in a collapse layer during the archaeological campaigns. Unfortunately, no evidence of the painted walls remained in their original location.

Four samples (PAT 1, 2, 3, 4; Table 1) come from the north-western side of the archaeological site, from a stratigraphic unit associated to the *domus* covered by 79 CE deposits (US 469, Fig. 1b). While other four fragments (PAS 1, 2, 3, 4; Table 1) were collected in the south-eastern side of the *villa* built after the 79 CE eruption (US 764, Fig. 1b), where probably a flight of stairs led to the upper floor. The pictorial surfaces of the fragments preserved bright colours both as monochrome backgrounds or refined decorations with geometric patterns and naturalistic motifs.

3. Methodological approach

Due to the different research aims associated with the study of painted walls, archaeometric investigations adopt a multi-analytical approach to determine various material components. Non-invasive and/or micro-destructive methods are mainly adopted in recent research [30–36] to characterise the pictorial layers (and pigments) from the compositional and mineralogical points of view, whereas underlying plaster layers are effectively studied by implementing microscopic and micro-analytical laboratory techniques to assess the

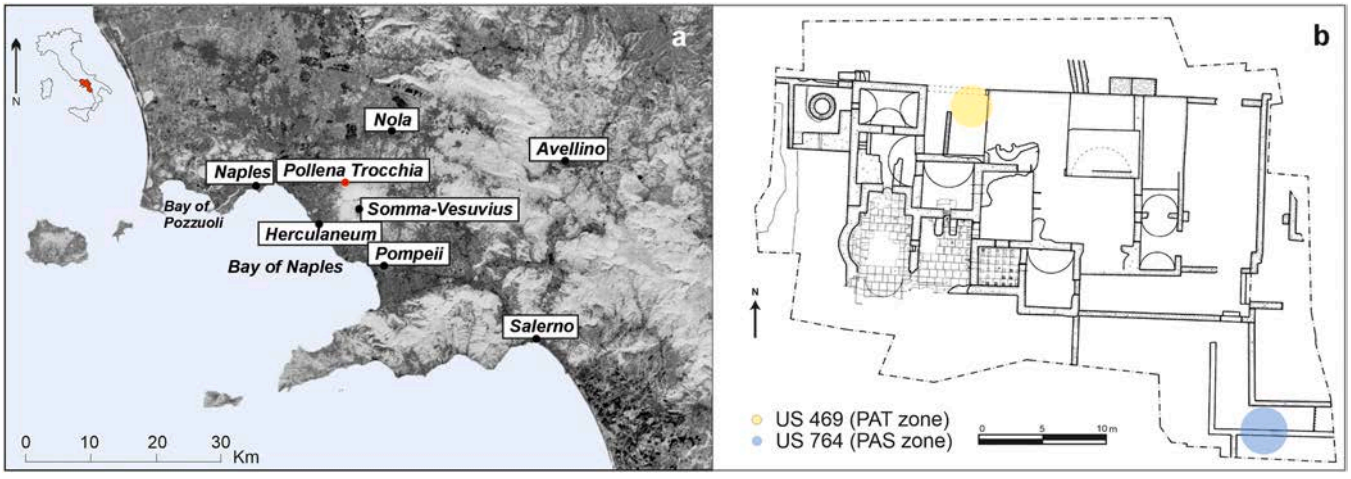

Fig. 1. a) Map of Vesuvian area reporting the location of Pollena Trocchia (red dot); b) plan of the archaeological site and US in which the samples were collected (modified from [29]).

Table 1
Macroscopic features of multi-layered plasters. Abbreviations: aren, arenaceous; conglomer, conglomeratic.

Date	US	ID Samples	Layers	Dimensional aspect	Colour	Cohesion	Thickness (mm)
Before 79 CE	469	PAT 1	Scratch coat	Arenaceous	Grey	Friable	< 2
			Arriccio	Arenaceous	Light Grey	Friable	12
			Intonachino	Aren.-conglomer.	White	Tenacious	5
			Painting	—	Red	—	< 1
	469	PAT 2	Scratch coat	Aren.-silty	Grey	Tenacious	< 2
			Arriccio	Arenaceous	Light grey	Tenacious	5
			Intonachino	Arenaceous	White	Friable	2
			Painting	—	Red/White/Green	—	< 1
	469	PAT 3	Scratch coat	Aren.-conglomer.	Grey	Friable	8
			Arriccio	Arenaceous	Light grey	Tenacious	5
			Painting	—	Red	—	ca. 1
	469	PAT 4	Scratch coat	Aren.-silty	Grey	Tenacious	< 2
			Arriccio	Aren.-conglomer.	Grey	Friable	13
			Intonachino	Arenaceous	White	Tenacious	ca 1.5
			Painting	—	Black	—	< 1
Between 79 and 472 CE	764	PAS 1	Scratch coat	Arenaceous	Light grey	Tenacious	12
			Arriccio	Silty	White	Tenacious	8
			Painting	—	Yellow	—	< 1
	764	PAS 2	*Arriccio*	Aren.-silty	Grey	Friable	7
			Intonachino	Aren.-silty	Light grey	Tenacious	6
			Painting	—	Blue	—	ca. 1
	764	PAS 3	*Arriccio*	Silty	Grey	Tenacious	14
			Intonachino	Arenaceous	White	Tenacious	8
			Painting	—	Purple/White/Green	—	< 1
	764	PAS 4	*Arriccio*	Arenaceous	Grey	Tenacious	12
			Intonachino	Arenaceous	White	Tenacious	8
			Painting	—	Green/Purple	—	< 1

mix-designs of supports.

In this perspective, the selected fragments were studied by a multi-analytical approach combining mineralogical and spectroscopic techniques; a flow chart detailing the methodological approach employed in connection with each specific research objective is provided in Fig. S1.

The samples were preliminary characterised by the macroscopic point of view (Table 1); then, the attention was focused on the pictorial surfaces in order to determine the nature of pigments used to decorate them.

The microscopic aspect of the surface was observed by means of Digital Microscopy (DM) using a Dino-Lite digital microscope with a magnification range of 400x - 470x, built-in coaxial illumination and Flexible LED Control (FLC), equipped 5.0-megapixel colour CMOS sensor. The acquisition of the images was performed by using the DinoCapture2.0 software.

Colour measurements were carried out by Fiber Optics Reflectance Spectroscopy (FORS), performed in the spectral range 380–1050 nm by a tungsten lamp (BeWTek, Inc. BPS101 Tungsten Halogen Light Source with a spectral output of 350 to > 2600 nm) as source and the grating Qmini Broadcom as detector. To investigate an area of 2 mm^2 a measuring head geometry of 45°/0° and a B&WTek inc. white plate (99%) as a reference were used. The measurement time for acquiring reflectance spectra and colorimetric coordinates (CIE L*a*b colour space) was of ca. 0.04 s (128 scans). For each colour, three measurements were carried out.

Chemical composition was obtained by X-Ray Fluorescence (XRF), carried out by a M1 MISTRAL Bruker XRF spectrometer with Rh target equipped with a silicon drift SDD detector (range of detection from Z > 13), using a voltage of 50 kV, a current of 800 μA, and a collimator size 0.5 × 0.5 mm.

Mineralogical information was obtained by using vibrational spectroscopic techniques; in particular, Raman spectroscopy (RS) was performed with a BRUKER BRAVO Handheld Raman spectrometer equipped with a charge-coupled device detector (CCD), using a Duo Laser excitation (785 and 853 nm) and a Sequentially Shifted Excitation technique (SSE™, patent number US8570507B1) for the fluorescence mitigation. Different measurement time was used in order to avoid saturation of the CCD. The Raman spectra were recorded in the spectral range between 178 and 3200 cm^{-1}. Raman analyses were supported by Fourier Transform Infrared Spectroscopy (FTIR) in Attenuated Total Reflectance (ATR) mode, carried out with a portable BRUKER Alpha FTIR spectrometer. The spectra were collected in a spectral range between 4000 and 400 cm^{-1} with resolution 4 cm^{-1} and 64 scans for each run. Bruker Opus 7.8 software was used for the acquisition and processing (i.e., baseline correction, smoothing) of both Raman and FTIR spectra.

The final phase of the study involved the collection of fragments for the preparation of thin- stratigraphic sections, so as to determine the mix-designs and type of raw materials adopted for making the supports and investigate the painting technique used for the application of pictorial layers onto the plaster substrate. Mineralogical assemblage, textural features of the plasters, and the support/pictorial layer interface were investigated by Polarized Light Microscopy (PLM) by using a Nikon Eclipse 6400 POL microscope equipped with a Nikon DS-Fi camera; microphotographs, acquired both in plane and crossed polarized light, were used for the determination of the Grain Size Distribution (hereafter GSD) by Digital Image Analyses (DIA); minimum Feret (mF) values were measured using ImageJ software. The minimum Feret value was used to calculate Krumbein φ (where $\varphi = -\log_2$ (mF)). Abundance of aggregate and the estimation of binder to aggregate ratio (B/A) were obtained by visual estimation [37].

4. Results and discussion

4.1. Wall paintings technology before 79 CE

4.1.1. Multi-layered plasters

Despite Vitruvius reported that plasters were characterised by seven different layers for covering the masonries of the ancient buildings [38], this assumption is not often verified, as generally the multi-layer technology provides on average three to four layers. The stratigraphy of the plasters from *Masseria de Carolis* consists of four layers (PAT 1, PAT 2 and PAT 4; Fig. 2a,b) whereas PAT 3 showed only three layers (Fig. 2c); the pictorial layer covered the outermost surface.

The three plasters layers of PAT 1, PAT 2 and PAT 4 were made with different mix designs, and we assigned the common nomenclature used

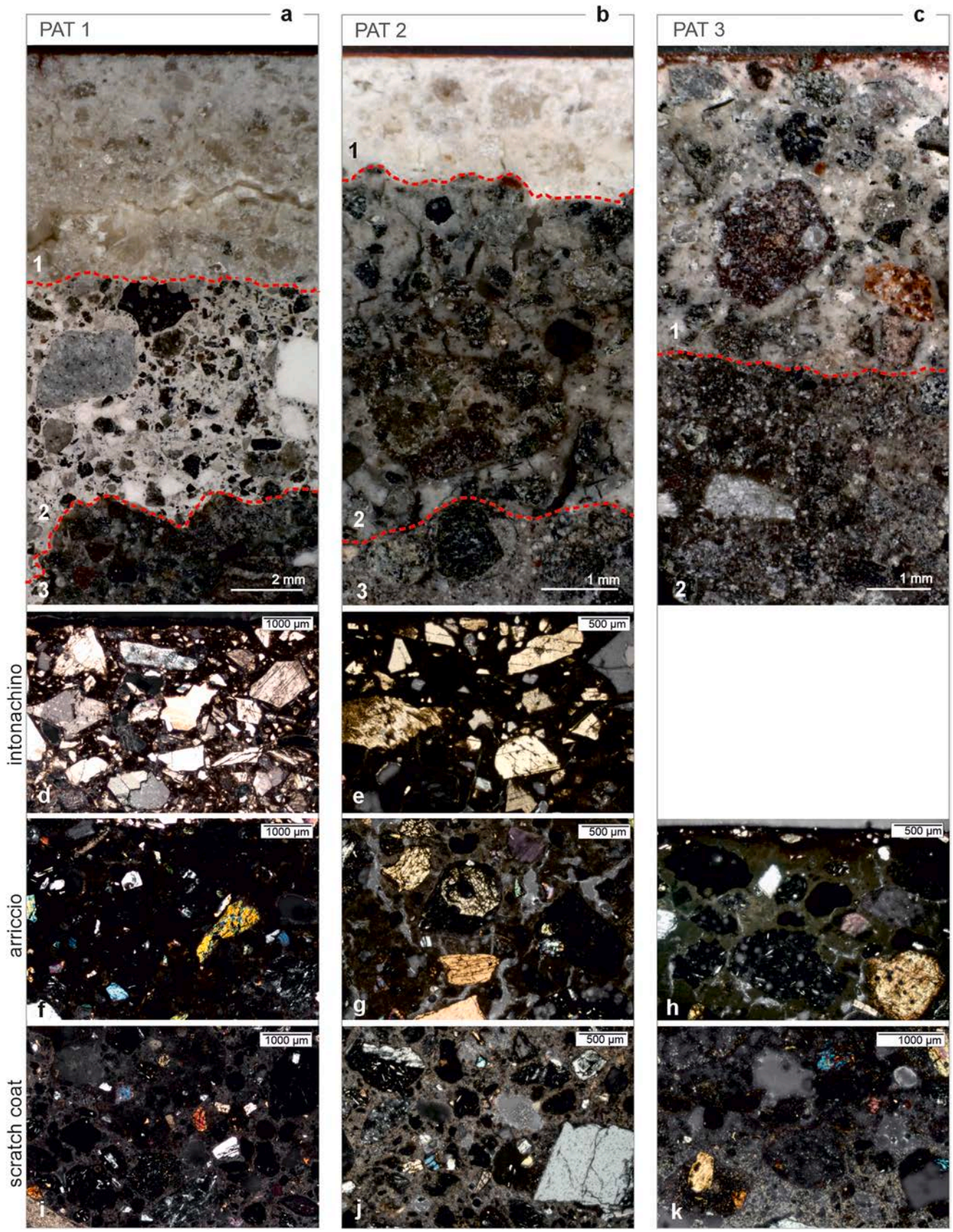

Fig. 2. Cross sections of multi-layered plasters of the *domus* covered by 79 CE eruption, observed via DM and PLM. DM image of PAT 1 (a), PAT 2 (b), and PAT 3 (c). Details acquired via PLM of the *intonachino* containing calcite crystals and marble dust (d, e), the *arriccio* containing volcanic sand (f, g, h), and scratch coat containing volcanic sand and showing unmixed lumps (i, j, k).

for plasters, from the top to the bottom: pictorial layer, *intonachino* (i.e., plaster s.s., the outermost layer beneath the mural painting), *arriccio* (i.e., rough coat layer intended to rectify the flatness and vertical mistakes), *rinzaffo* (i.e., scratch coat layer constituting the anchorage element to the masonry) [39]. A lexicon table is provided in the Supplementary material (Table S1).

Intonachino was a layer composed by cryptocrystalline and isotropic lime binder, with frequent unmixed lumps, in which aggregate (with B/A ratio ranging from 1.0 to 1.8; Table 2) was composed by heterometric (average φ_{mF} from 3.6 to 4.1; Table 2), angular crystals of sparry calcite and marble fragments (*marmorino*) (Fig. 2d). The presence of sand-sized/calcite-bearing aggregate (Fig. 2e) attests the deliberate addition of such a type of component for rendering a neutral colour, serving as support for the pictorial layer [11,22,39–42]. It was thicker in the sample PAT 1 (6 mm) and appeared thinner in PAT 2 and PAT 4 (2–1.5 mm; Table 1). As observed in other contexts [18,43], the addition of marble dust (*marmorino*) represents an appropriate technological choice, also suggested by Vitruvius, who recommended its use for a shine and lustre appearance of the plaster and, at the same time, for increasing its cohesiveness and mechanical properties [38].

Underneath the *intonachino*, a layer (5–13 mm; Table 1) composed by a cryptocrystalline and birefringent binder with scattered rounded volcanic grains (*arriccio*) (Fig. 2f,g) was observed. The aggregate (ca. 35–40%) was composed by prevalent juveniles (scoriae, leucite-bearing scoriae, pumices) along with lower crystals of clinopyroxene, sanidine, plagioclase, and traces of amphibole, biotite, olivine. The mineralogical assemblage of such a volcanic sand is consistent with the Somma-Vesuvius volcanics used as pozzolanic addition also in other contexts of Campania and other regions alongside with the pozzolana s.s., coming from the Phlegraean Fields [19,20,44,45].

The aggregate showed pozzolanic reaction rims (Fig. 2h) that indicate the interaction between the Si- and Al- rich materials with calcium hydroxide to form calcium silicate hydrates (C-S-H or C-A-S-H phases) to improve the hydraulic properties of the binder [40,46]. The aggregate of *arriccio* layers was coarser (average φ_{mF} from 0.99 to 1.12) and less abundant (B/A= 1.8) in PAT 2 and PAT 4, where the juveniles predominated and only scarce crystals were observed. Moreover, in the sample PAT 1 rare crystals of calcite and limestone fragments were also observed (Table 2).

The *arriccio* laid on the scratch coat that adhered on the masonries. *Arriccio* and scratch coat share the same volcanic aggregate; however, the microcrystalline and anisotropic lime binder of these layers includes frequent unmixed lumps (Fig. 2i,j). The incorporation of pozzolanic additives not only conferred hydraulic properties to the mortar but also improved wall adhesion and accelerates the setting time [39].

On the other hand, the sample PAT 3 shows only three layers (Fig. 2c). The *intonachino* lacks, and only sporadic small crystals of calcite are incorporated in the pictorial layer. Below the pictorial layer, plaster layers, characterised by mix-designs consistent with the *arriccio* and scratch coats of the other samples, were observed (Fig. 2h,k; Table 2).

4.1.2. Pigments

White. In the decorated plasters collected from the US 764, white (Fig. 3) was observed both as background colour and as pigment for drawing details (Fig. 4). The fragments, in fact, showed white decorations on darker painted layers (dark red in PAT 3, black in PAT 4; Figs. 4, 5) whereas a white background features PAT 2 (Fig. 4), on which more complex decorative motifs were present (Fig. 6a).

Chemical analyses performed on the white surfaces revealed the presence of Ca along with traces of Sr (Table 3) associated to carbonates, as highlighted by ATR-FTIR and Raman spectra (Table 3; Fig. 3). In particular, the acquired spectra revealed that white details on black

Table 2
Minero-petrographic characterisation of multi-layered plasters by PLM. Abbreviations: crypt, cryptocrystalline; micr, microcrystalline; isotr, isotropic; anisotr, anisotropic; pum, pumices; sc, scoriae; afs, alkali feldspar; pl, plagioclase; cpx, clinopyroxene; ol, olivine; amp, amphibole; cal, calcite; bt, biotite; CF, carbonate fragments; MD, marble dust; Av. φmF, average phi minimum Feret; S(φmF), standard deviation of φmF; tr, traces.

Date	ID Samples	Layers	Binder texture	Minerology of aggregate	Aggregate (%)	B/A	GSD				Lumps
							max (mm)	min (mm)	Av. φmF	S (φmF)	
Before 79 CE	PAT 1	Scratch coat	Isotr., Crypt.	Sc, Pl, Cpx, Afs	40	1.5	0.83	0.03	3.3	0.90	Frequent
		Arriccio	Isotr., Crypt.	Pum, Sc, Pl, Cpx, Ol, Afs, Cal, CF	40	1.5	0.79	0.03	3.2	0.83	Frequent
		Intonachino	Isotr., Micr.	Cal, MD	50	1.0	0.74	0.02	3.6	1.03	Absent
	PAT 2	Scratch coat	Isotr., Crypt.	Sc, Afs, Pl, Cpx	40	1.5	1.28	0.02	3.3	1.22	Absent
		Arriccio	Isotr., Crypt.	Sc, Pum, Pl, Afs, Cpx, Bt (tr)	35	1.8	0.77	0.03	3.1	1.12	Rare
		Intonachino	Isotr., Crypt.	Cal, MD	35	1.8	0.22	0.01	4.1	0.90	Absent
	PAT 3	Scratch coat	Anisotr., Micr.	Sc, Lc, Pl, Cpx, Afs	30	2.3	0.97	0.08	1.9	0.93	Rare
		Arriccio	Isotr., Crypt.	Cal, Sc, Cpx	30	2.3	1.19	0.03	2.3	0.99	Rare
	PAT 4	Scratch coat	Anistr., Micr.	Sc, Pum, Pl, Afs, Cpx, Amp	40	1.5	0.51	0.06	2.7	0.65	Present
		Arriccio	Isotr., Crypt.	Sc, Pum, Pl, Afs, Cpx, Amp	35	1.8	0.74	0.04	2.7	0.99	Present
		Intonachino	Isotr., Crypt.	Cal, MD, Sc(tr)	35	1.8	0.34	0.01	3.6	1.10	Absent
Between 79 and 472 CE	PAS 1	Scratch coat	Anisotr., Micr.	Sc, Pum, Cpx, Pl, Afs, Bt (tr)	35	1.8	0.79	0.03	3.2	0.83	Present
		Arriccio	Isotr., Crypt.	Sc, Cpx, Pl, CF	35	1.8	0.99	0.06	2.5	0.97	Frequent
	PAS 2	*Arriccio*	Anisotr., Micr.	Sc, Pl, Cpx	30	2.3	1.01	0.06	2.2	0.89	Present
		Intonachino	Isotr., Crypt.	CF, Cal	35	1.8	1.37	0.08	1.8	0.96	Present
	PAS 3	*Arriccio*	Anisotr., Micr.,	Sc, Pum, Cpx	30	2.3	1.27	0.05	2.4	0.96	Frequent
		Intonachino	Isotr., Crypt.,	CF, Cal(tr)	35	1.8	0.83	0.06	2.5	0.95	Frequent
	PAS 4	*Arriccio*	Anisotr., Micr.,	Pum, Sc, Cpx, Afs, Pl, Bt	35	1.8	0.05	0.05	2.4	1.09	Frequent
		Intonachino	Isotr., Crypt.,	CF	35	1.8	1.06	0.05	2.1	1.19	Frequent

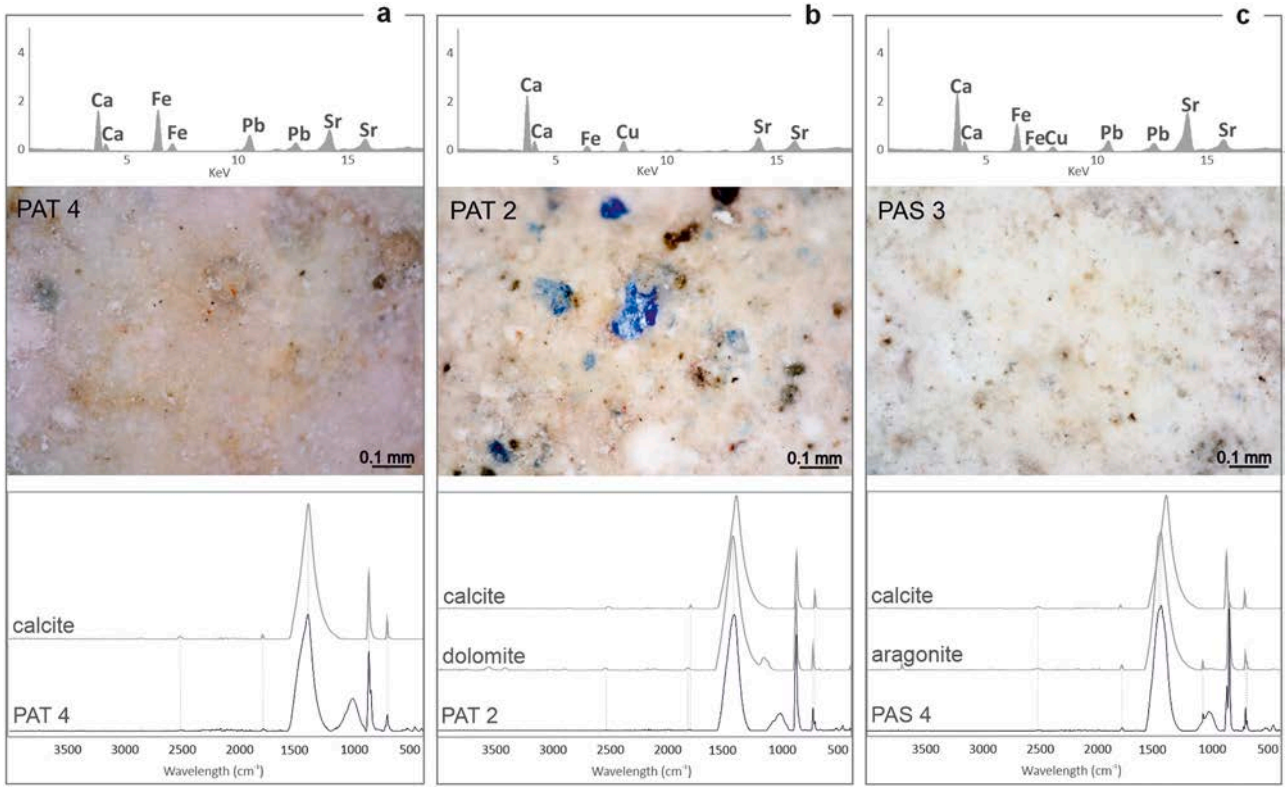

Fig. 3. DM images and spectroscopic data of white painting layers observed in the samples PAT 4 (a), PAT 2 (b) and PAS 3 (c) (reference infrared spectra from RRUFF database).

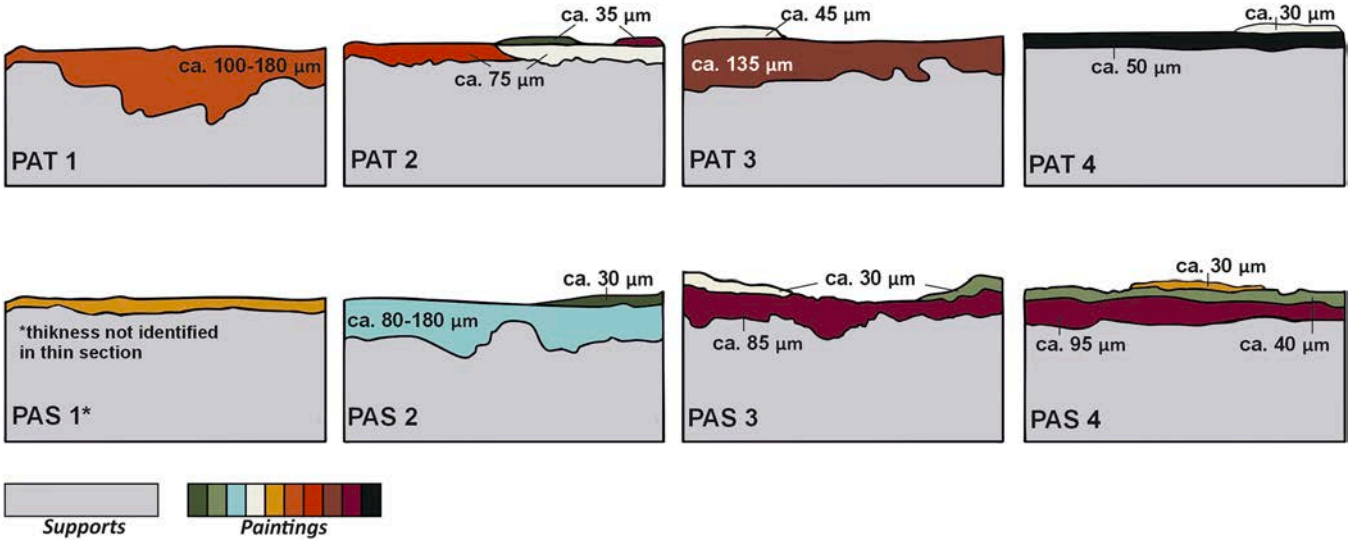

Fig. 4. Cross section sketch with pictorial layers and their thickness.

decoration of PAT 4 were obtained only by calcite (Fig. 3a) whereas white background in the sample PAT 2 and the white stripe of PAT 3 were obtained by using a mixing of calcite and dolomite (Table 4; Fig. 3b).

FTIR and Raman spectroscopy turned out to be appropriate methods for the identification of carbonate phases differing in crystallographic structure and chemical composition. The peaks due to their characteristic bonds, in fact, slightly shifted in relation to the type of carbonate under investigation (e.g. [47–49]).

White details of PAT 4 showed the typical features of calcite (ATR-FTIR: 1793, 1404, 872, 711 cm^{-1}; Raman: 1087 cm^{-1}; Table 3). They were also observed in the white stripe of PAT 3 and on the white background of PAT 2 along with those of dolomite, as highlighted by the presence of the peak at 729 cm^{-1} on the ATR-FTIR spectrum [49] and the characteristic Raman shifts at 1097 and 298 cm^{-1} (Table 3; Fig. 3b). As with infrared spectroscopy, Raman peaks positions are influenced by the magnesium content. In particular, the substitution of Ca^{2+} with the smaller Mg^{2+} ion in the cell increases the inter-atomic distances; thus, the increase of Mg content determines the shift of Raman peaks toward higher values [50].

Moreover, DM observation also highlighted the presence of scattered blue crystals in PAT 2 (Fig. 3b) and XRF detected traces of Cu, suggesting

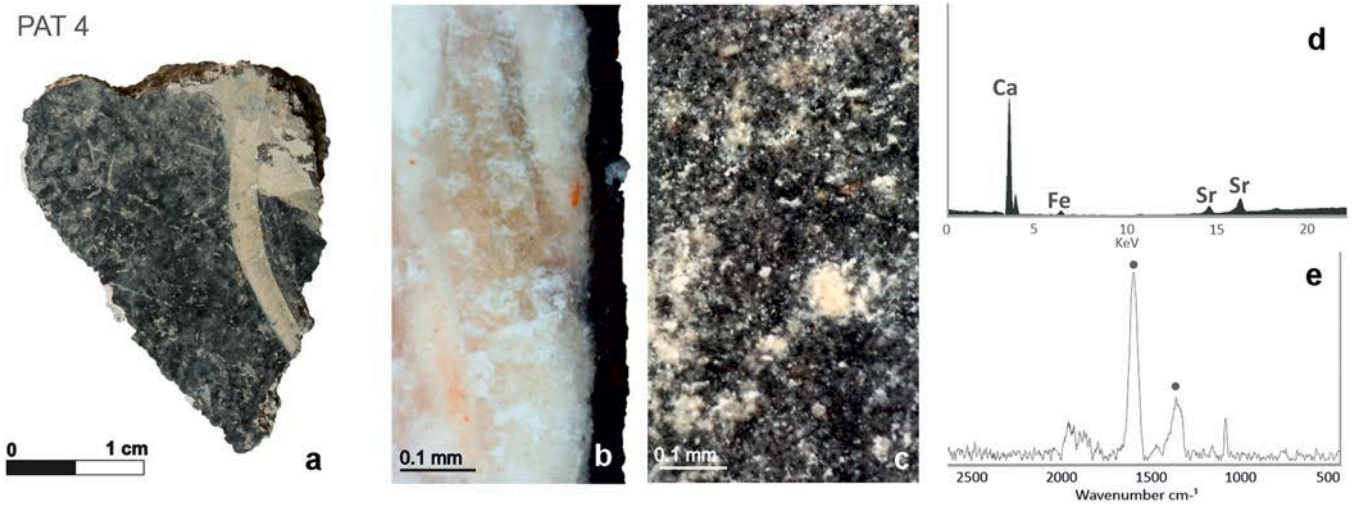

Fig. 5. Sample PAT 4 (a) featured by a black surface, observed by DM in cross-section (b) and on the surface (c), where white and rare red particles were also observed. XRF (d) and Raman (e) spectra.

the addition of a copper-based (Egyptian) blue pigment, likely to create a more brilliant background [41].

Black. The black pigment was observed as background in the sample PAT 4 (Figs. 4, 5a). DM showed a compact surface on which white particles and red crystals were observed (Fig. 5b, c). XRF reported the presence of Ca and Fe along with traces of Sr (Table 3; Fig. 5d). ATR-FTIR spectrum only detected the presence of calcium carbonate (Table 3), probably due to the medium in which the pigment was dispersed or signals from the *intonachino* [51]. RS revealed the nature of the pigment, displaying the diagnostic shift of carbon black at 1390 and 1615 cm^{-1} (Table 3; Fig. 5e) [52,53]. This type of pigment, largely diffused since the Prehistoric age [54], was obtained from the incomplete combustion of organic material [55].

Red. Red colour was observed in three different shades (Fig. 6a-c), from bright to darker hues, as confirmed by colorimetric data (Table 3). More brilliant red (L*= 63.45; a*= 38.13; b*= 29.78) observed on the surface of sample PAT 2 (Fig. 6a) was characterised by red matrix in which rare white and brown-black particles were scattered. XRF analysis (Fig. 6d) revealed the presence of Ca, Fe and Hg, along with traces of Sr and Pb (Table 3). Raman spectrum showed the peaks at 253, 283, 343 cm^{-1}, confirming the use of cinnabar (HgS) [56]. Also reflectance spectra obtained by FORS are consistent with the cinnabar spectrum, showing very sharp positive slope near 600 nm (Fig. 6e) [4].

The decoration of this sample is of exceptional quality considering the scarce availability of the pigment, which made it more expensive (it costed even triple the amount of popular pigments, as established by Roman law) and affordable only for the elite that were able to decorate walls in the most expensive colour [51,57]. For this reason, the painting in red with cinnabar was often used for decorations of higher artistic value, as the decoration of this sample (Fig. 6a).

Despite its preciousness, this pigment tends to darken up to black under solar irradiation [58,59], an effect that was usually prevented by the dilution of cinnabar with red earth [51]. In fact, the Romans were aware of this colour change and used the pigment manly for decoration inside, away from direct sunlight. The process is mainly due to the exposure to direct sunlight (or even moonlight [60]); however darkening is also prone to other different factors, such as atmospheric agents and associated pollutants, relative humidity, soluble salts and organic compounds, that accelerate the blackening effect due to the oxidation of the sulphur (determining the phase transition to black metacinnabarite), or other chemical reactions mainly attaining with the presence of specific components (e.g. chlorine or other halogens) [61,62]. In our case, the preservation of the vibrant red hue could suggest the development of burial conditions that unaffected its vivid colour.

A lighter shade of red (L*= 61.32; a*= 28.39; b*= 25.42) was observed on PAT 1 (Fig. 6b). The dimension of grains on this surface was evidently coarser than the previous red hue; moreover, some white and black particles were also noted (Fig. 6b). XRF revealed the presence of Fe and Ca and traces of Sr and Pb (Fig. 6d). Absorption bands at 535 and 460 cm^{-1} characteristics of iron oxides are present in ATR-FTIR spectrum (Table 3; Fig. 6f) and Raman peaks are characteristic of hematite (α-Fe_2O_3) (612, 412, 293 cm^{-1}; Table 3). These results are confirmed by the soft sigmoid-shape FORS curves, with a characteristic maxima reflection near 630 nm and 750 nm and an absorption band around 550, 660 and 850–900 nm, attributable to the red ochre (Table 3; Fig. 6e) [63,64]. The presence of Pb suggests the possible addition of lead-based red pigment (i.e. *minium*) according to a recipe widely employed by Romans [17].

The same pigments were mixed also to obtain the darker red shade (L*= 51.78; a*= 16.67; b*= 11.28), as observed in PAT 3 (Fig. 6c). The red surface seems to be darkened by the abundant presence of black particles, which could be attributable to an addition of black pigment, whose nature was not properly revealed by the analyses performed so far. However, they could be due to the presence of organic black particles or to Pb-rich pigment, the latter notoriously instable. XRF detected Fe, Ca, traces of Sr and Pb (Table 3; Fig. 6d), that can be justified as the addition of *minium* to an Fe-rich pigment to darken the final colour. Spectroscopy identified iron oxides with the typical infrared bands at 533 and 462 cm^{-1} (Fig. 6f), and the Raman shifts characteristic of hematite (Table 3) [65]. Moreover, the FORS spectrum is typical of hematite, despite a less marked slope near 550 nm (Fig. 6e), probably influenced by darker pigment mixture.

Purple. Purple pigment (L*= 62.46; a*=12.68; b*= 9.10) was observed on a thin band decoration on the PAT 2 (Figs. 4, 6a). XRF detects the presence of Fe, Ca, a lower content of Pb, Cu and Sr and traces of K and Mn (Table 3). Concerning the spectroscopic measurement, IR bands at 543, 466 cm^{-1} are attributable to iron oxides, and Raman peaks at ca. 415, 298, 225 cm^{-1} (Table 3) are consistent with hematite. The presence of hematite as chromophore influences the reflectance spectral features with the characteristic S-shape [66].

It is interesting that, to obtain the purplish hue, hematite was mixed with other substances; in fact, DM disclosed the presence of blue crystals, thus illuminating on the occurrence of Cu in XRF spectra (Table 3). The mixture of hematite, likely in coarser grains considering the darker

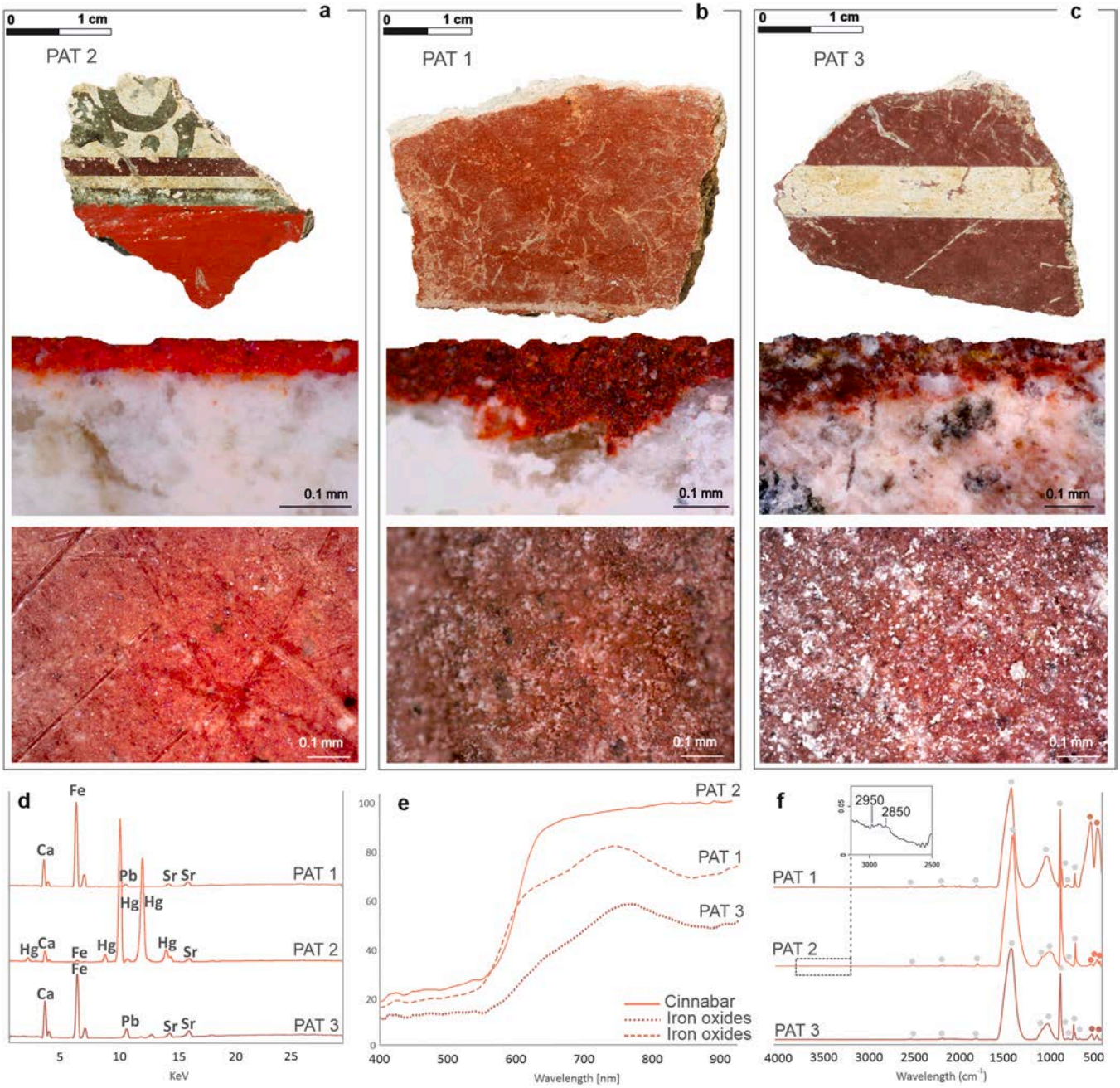

Fig. 6. Red hues observed on PAT 2 (a), PAT 1 (b), PAT 3 (c) samples, observed in cross-sections and on the painted surfaces by DM. Comparison between XRF spectra (d), reflectance curves by FORS (e) and ATR-FTIR spectra (f) with a zoom of range 2500–3000 in the dotted box (PAT 2 sample).

shade [40,67], along with blue pigment, in particular Egyptian blue, was already reported by ancient authors, and was also well documented in different archaeological contexts [41,68–70]. Finally, the detection of Pb in the mixture could again suggest the addition of *minium*.

Green. Some green details (L*= 73.36; a*= −1.85; b*= 10.26) were observed on PAT 2 (Fig. 6a). Pliny reported various recipes used by ancient painters to obtain green hues [60]. Actually, Roman painters were fairly familiar with the use of different green pigments, such as malachite, verdigris, chrysocolla, and green earths, the latter also called *Creta viridis* and described by the author as unsuitable for the wall decoration [60].

As far as the green pigment is concerned, Ca, Fe, Sr, and traces of K and Mn, along with Cu were measured by XRF (Table 3). It is worth noting that the presence of Cu is compatible with the observation of blue crystals scattered in the green matrix, again suggesting the mixing of green pigment with a copper-based blue (Table 4). Unfortunately, Raman signals are strongly affected by fluorescence effects; however, all the spectroscopic data converge to the use of green earths, a natural mixture of iron oxides, clays, and silicates, in which the commonest are glauconite and celadonite, minerals belonging to the clayey micas group [71]. In particular, FORS displayed a reflectance maximum near 550 nm [66], and ATR-FTIR spectrum showed diagnostic infrared bands allowing us to recognize celadonite (Table 3).

Although the different geological origin (celadonite occurs in volcanic rocks, glauconite in sedimentary rocks), the two minerals have a very similar chemical composition, therefore, their distinction is quite difficult. However, recent works [69,72,73] allowed for a more precise identification by the comparison of the vibrational features, providing more detailed and necessary information for the study of the pigments

Table 3
Results of multi-analytical techniques performed on the pictorial layers.

Date	ID Sample	Painting Colour	Stratigraphic position	Colorimetric coordinates L* (D65)	a* (D65)	b* (D65)	RGB colours	XRF	ATR-FTIR (cm^{-1})	Raman (cm^{-1})	FORS (nm)
Before 79 CE	PAT 1	light red	background	61.32	28.39	25.42		Fe, Ca, Sr, Pb	2510, 1794, 1411, 1030, 872, 855, 797, 712, 535, 460	612, 412, 293	~630, ~750
	PAT 2	brilliant red	superficial decoration	63.45	38.13	29.78		Hg, Ca, Fe, Sr	2950, 2851, 2512, 1794, 1406, 1080, 992, 873, 800, 712, 528, 469, 439	253, 283, 343	~600
		white	background	84.40	2.13	14.93		Ca, Fe, Sr, Cu	2522, 1820, 1795, 1417, 875, 729, 713	—	—
		green	superficial decoration	73.36	-1.85	10.26		Ca, Fe, Cu, Sr, Mn, K	3557, 3530, 1640, 1109, 1073, 960, 872, 854, 796, 680	—	~550, ~810
		purple	superficial decoration	62.46	12.68	9.10		Fe, Ca, Pb, Sr, Cu, Mn, K	2514, 1980, 1794, 1410, 1157, 1030, 1014, 873, 794, 729, 712, 543, 466	417, 298, 226	~630, ~780
	PAT 3	dark red	background	51.78	16.67	11.28		Fe, Ca, Pb, Sr	1794, 1405, 1163, 1030, 873, 796, 778, 712, 643, 532, 460	612, 412, 293	~650, ~760
		white	superficial decoration	82.65	4.57	17.53		Ca, Fe, Sr, Pb	2525, 1820, 1795, 1418, 874, 729, 713	1097, 298	—
	PAT 4	black	background /superficial decoration	43.52	-0.25	0.08		Ca, Fe, Sr	2513, 1794, 1404, 1023, 872, 712, 474	1615, 1360	—
		white	background	74.85	1.75	10.32		Ca, Fe, Sr, Pb	2513, 1793, 1405, 872, 712	1097, 1087	—
Between 79 and 472 CE	PAS 1	yellow	background	76.51	12.06	37.34		Fe, Ca, Sr	3694, 3617, 2513,1794, 1408, 1164, 1029, 912, 795, 712, 627, 535, 467, 430	568, 385	~600, ~760
	PAS 2	blue	background	80.21	-6.79	-2.67		Cu, Ca, Pb, Sr, Fe	1981, 1795, 1417, 1158, 1047, 1004, 872, 792, 755, 730, 712, 663, 593, 563, 520, 478, 422	—	~500, ~730
		green	superficial decoration	86.92	-12.79	16.49		Ca, Fe, Cu, Sr, Mn, K	3556, 3531, 1635,1073, 958, 872, 854, 798, 680		~550, ~810
	PAS 3	purple	background	53.95	13.92	4.40		Fe, Ca, Pb, Sr, Cu, Mn, K	2514, 1980, 1794, 1410, 1157, 1030, 1014, 873, 794, 729, 712, 543, 466	417, 298, 226	~630, ~780
		green spot	superficial decoration	62.77	-10.05	20.57		Fe, Ca, Pb, Cu, Sr	—	—	~550, ~810
		white	superficial decoration	89.43	1.60	9.15		Ca, Sr, Fe, Pb, Cu	2508, 1787, 1466, 1448, 874, 853, 713, 700	—	—
	PAS 4	green	superficial decoration	64.90	-7.07	10.23		Fe, Ca, Pb, Cu, Sr	3554, 3530, 1640, 968, 872, 854, 798, 680	—	~550, ~810
		purple	background	56.27	17.58	5.58		Fe, Ca, Pb, Sr, Cu, Mn, K	2514, 1980, 1794, 1410, 1157, 1030, 1014, 873, 794, 729, 712, 543, 466	417, 298, 226	~630, ~780
		yellow spot	superficial decoration	80.67	7.32	29.98		—	—	—	~600, ~760

Table 4
Synoptic table reporting the recipes of multi-layered plasters and pigments.

	Before 79 CE	Between 79 and 472 CE
Plasters	**Scratch coat** lime plasters with volcanic aggregate ***Arriccio*** lime plasters with volcanic aggregate ***Intonachino*** lime plasters with calcite and marble dust as aggregate	- ***Arriccio*** lime plasters with volcanic aggregate ***Intonachino*** lime plasters with calcite and organogenic limestones as aggregate
Pigments	**Red** red ochre, cinnabar, red ochre + red lead **White** calcite, calcite + dolomite **Green** green earths + egyptian blue **Purple** hematite + red lead + egyptian blue **Black** carbon black - -	- **White** calcite + aragonite **Green** green earths **Purple** hematite + red lead + egyptian blue - **Yellow** yellow ochre **Blue** egyptian blue

used in archaeological materials.

In our plaster, the narrow bands at 3557 and 3530 cm^{-1} (stretching vibrations of the hydroxyl groups), along with the stretching vibration within the tetrahedral sheet at 1109 (Si–O vibration perpendicular to SiO_4 tetrahedral sheet), 1073 and 960 cm^{-1} (in-plane Si–O stretching vibration) and the bands at 796 and 680 cm^{-1} given by OH bending vibration involving octahedral cations (Table 3), attested the use of celadonite [72–74].

4.1.3. Painting techniques

The samples from the *villa* exhibit different painting techniques, and all reveal lime as the only binder. These techniques include *fresco*, *mezzo-fresco* or lime painting.

The *fresco* painting technique, based on the application of a suspension of pigments in water on a fresh and water-saturated mortar [75–77], usually presents pictorial layers in stratigraphic continuity with the plaster and has a very subtle thickness directly related to the grain size of the pigment used [76]. The *mezzo-fresco*, instead, requires an almost but not quite dry plaster, and the use of a limewater pigment suspension. More generally, lime-based techniques involve the application of pigments mixed with limewater or even slaked lime after the complete drying of the plaster. In these techniques the pigment-bearing layer shows a variable discontinuity with the underlying plaster and is generally thicker than in the pure *fresco* paintings. Additionally, the thickness varied considerably according to the skill and needs of the painter [76]. All these techniques were used widely in the Roman world and in particular the fresco technique had the capacity to make the wall painting stable and resistant over time [8,43].

Red pigments (on PAT 1, PAT 2, PAT 3; Fig. 6) show borderline conditions between a purely *fresco* painting technique and a lime-painting technique. In particular, there are interactions between the paint layer and the plaster, i.e., pigment particles penetrating the first layer of the plaster (Fig. 6a), which is impossible with a substrate that has fully hardened. Nevertheless, the thickness of the paint layers is much thicker (Fig. 4) than the grain size of the pigment detected and often appears to be mixed with white portions of a probable carbonate nature (calcite) (Fig. 6a-c). These layers were probably applied using the *mezzo-fresco* technique on a partially hardened substrate and with the use of a limewater suspension.

It is remarkable to notice that the red cinnabar on PAT 2 presents a glossy surface (Fig. 6a). ATR-FTIR spectrum actually reported absorption bands between 2950 and 2850 cm^{-1} related to C–H stretching vibration (Fig. 6f) attributable to organic material [78]. Having said that, a more accurate observation and the analyses of the pigment have allowed us to infer that the organic compound could represent a thin film coating the red pictorial layer, as commonly performed to protect and enhance the vibrancy of the cinnabar red colour [58–60,79].

On the same fragment even the white pigment (plus Egyptian blue) was applied by *mezzo-fresco* technique, while the superimposed green plant motifs and purple bands were painted by using a different technique. Hence, the pictorial layer was clearly divided by the underlying sublayer suggesting the application of pigment by means of a lime-based painting technique, in particular with the application of a pigment suspension based on slaked lime.

It is worth noting that the same technique has been observed for the black colour on PAT 4 (Fig. 5b) and for decorative details on PAT 3 (Fig. 6), allowing to hypothesize that the lime-based technique was related to the application of decorative motifs.

4.2. Wall paintings technology between 79 and 472 CE

4.2.1. Multi-layered plasters

Plasters sampled from the ceiling of the *villa*, occasionally preserving the *incannucciata* (reed leaves wattle) imprints on the back of the plaster, are characterised by textural and mineralogical features suggesting different technological choices with respect to the wall painting technology used to cover the masonries of the pre-79 CE *villa*.

All samples are characterised by the presence of three layers, although PAS 1 showed different mix-designs (Fig. 7a). The latter, similarly to the sample PAT 3, shows a basal layer characterised by the presence of volcanic aggregate (scoriae, pumices, clinopyroxene, plagioclase, amphibole, olivine) (35%) in a microcrystalline and birefringent binder with frequent unmixed lumps (Table 2; Fig. 7a). Upon this surface, a layer of a cryptocrystalline, anisotropic binder mixed to volcanic aggregate was observed (Fig. 7a). Although it was poorly preserved in the thin section, the nature and the abundance (B/A ratio in the amount of 1.8; Table 2) were clearly visible via DM (Fig. 7a).

On the other hand, PAS 2, PAS 3 and PAS 4 are characterised by an *arriccio* layer consisting of a pale grey microcrystalline and birefringent binder mixed to volcanic aggregate (B/A between 2.3 and 1.8) composed by scoriae, pumices, small crystals of plagioclase and clinopyroxene, bordered by evident reaction rims (Table 2; Fig. 7b). The *intonachino* layer was made by adding to the microcrystalline and birefringent lime binder an aggregate (B/A ratio = 1.8) consisting of sporadic calcite crystals and abundant, rounded limestone fragments containing microfossils (Fig. 7b). Frequent unmixed lumps were observed in both layers (Table 2; Fig. 7b).

The variations in composition and quantity of aggregates found in the plasters of the older building suggest the use of different raw materials. Specifically, the volcanic aggregate is likely sourced from selected Vesuvian sands, while the distinct characteristics of carbonate-bearing aggregates of the *intonachino* indicate potential variations in their geological origin.

4.2.2. Pigments

White

The analyses performed on white band observed on PAS 3, which are featured by a purple decoration and a green spot (Figs. 4, 8a), revealed interesting information about the diachronic use of different white pigments. Although XRF detected Ca and Sr along with Fe, Pb, and Cu, due to the underlying colours, ATR-FTIR revealed the presence of aragonite along with calcite (Table 3; Fig. 3c). Infrared spectrum, in fact, presents the peak due to the deformation of the planar ion CO_3^{2-} at 853 cm^{-1}, diagnostic of this $CaCO_3$ polymorph [49,80], whose association with calcite could be due to the mixing in the preparation of the colour from lime-based medium used to dilute and apply the pigment (see next paragraph).

It was proved that aragonite became the predominant white pigment

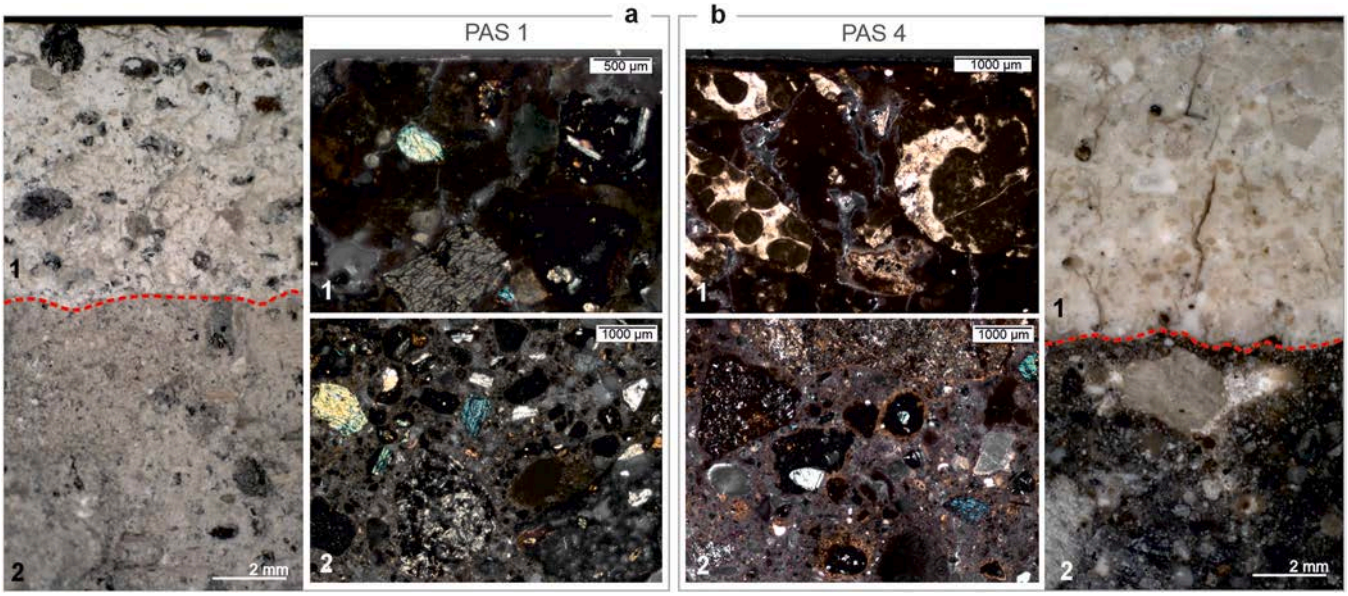

Fig. 7. Cross-sections of multi-layered plasters of the *villa* built on 79 CE eruption deposits, observed via DM and PLM. a) DM images of PAS 1 and details in PLM of volcanic sand used in the layers 1 and 2; b) DM images of PAS 4 and details in PLM showing limestone fragments containing microfossils in the *intonachino* (1) and volcanic aggregate with evident reaction rims in the *arriccio* (2).

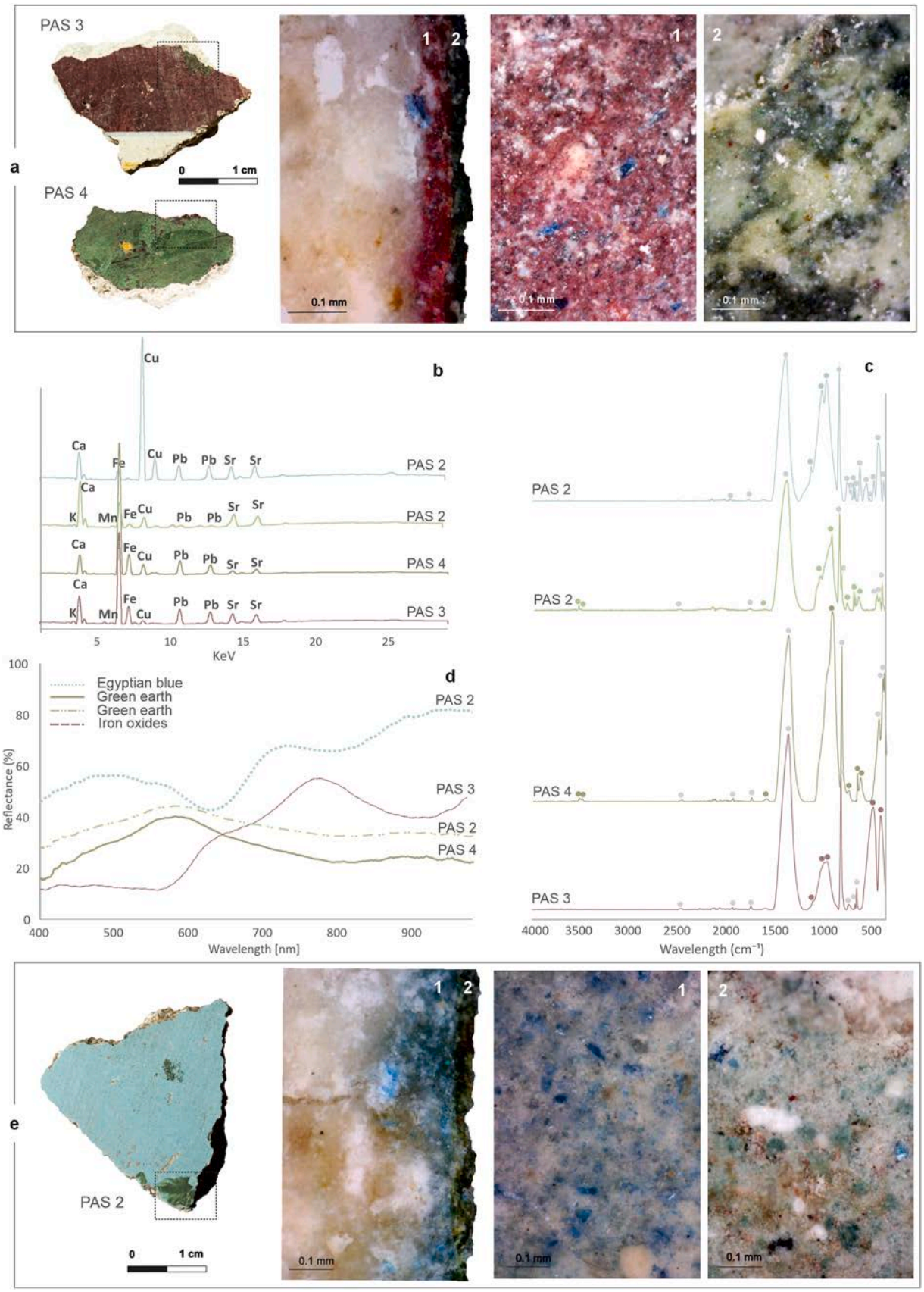

Fig. 8. Multi-layered paintings of PAS 3 and PAS 4 (a) samples; comparison between XRF (b), ATR-FIR (c) and FORS (d) spectra, also including the blue and green pictorial layers visible on PAS 2 sample (e).

during the Imperial period, instead of calcite and dolomite more popular in the Augustan period [47]. Studies performed on several Roman wall paintings, in fact, permitted the intriguing correlation between the type of white pigment, the period of execution and quality of the painting [47]. The reason of the large diffusion in the use of pigment could lie in a greater availability of *creta calcarea* [57,81], a white earth containing aragonite imported from Egypt and Greece in that period [82] that reached Mediterranean coasts due to new exchange routes or new artistic tastes. Moreover, other technical reasons were invoked, as the selection of a more specific white pigment and/or the increasing use of *mezzo-fresco* and *secco* techniques [83].

This is consistent with the results obtained on the analysed samples from *Pollena Trocchia*, since whites in plasters from the pre-79 CE *villa* are composed of calcite and dolomite whereas the white pigment used in the *villa* dated back in-between 79 and 472 CE is aragonite (Table 4).

Moreover, the use of aragonite undeniably indicates a refinement of the decoration (likely) highlighting a high rank of the patrons, as also suggested by some structural elements (i.e. baths) [47].

Purple

The purple hue was analysed on PAS 3 (L*= 53.95; a*= 13.92; b*= 4.40) and beneath the green layer of sample PAS 4 (L*= 56.27; a*= 17.58; b*= 5.58; Table 3; Figs. 4, 8a).

The presence of hematite was highlighted by Fe peak in XRF (Fig. 8b), the ATR-FTIR adsorption bands at 543 and 466 cm^{-1} (Fig. 8c), Raman shifts (ca. 417, 298, 226 cm^{-1}; Table 3), and S-shaped curve by FORS (Fig. 8d) [66]. The detection of Pb suggests the addition of a lead-based red pigment; in addition, Cu peak detected by XRF (Fig. 8b) confirmed the mixing of crystals of Egyptian blue observed by DM and PLM (Fig. 8a), along with its typical absorption infrared bands at ca. 1159, 1040 and 1005 cm^{-1} (Fig. 8b).

Whole data of the purple pigment report a mixture of Fe and Pb -based red pigments and Egyptian blue matching the pigment used for decorating the older *domus* (sample PAT 2; Table 3).

Green

Green decoration observed on decorated plasters from the *villa* were obtained by using the same pigment adopted for drawing details on wall paintings of the *villa* buried by 79 AD eruption.

Analyses of green pigment, used extensively in PAS 4 (L*= 64.90; a*=−7.07; b*= 10.23) and in details of PAS 2 (L*= 86.92; a*= −12.79; b*= 16.49) and PAS 3 (L*= 62.77; a*= −10.05; b*= 20.57), still revealed, in fact, the use green earths (Table 3), mixed to Egyptian blue in PAS 3 and PAS 2 (Fig. 8a,e).

In fact, XRF detected Fe, Ca, Sr, Pb and Cu, with traces of K and Mn in sample PAS 2 (Table 3; Fig. 8e). Although Pb and Cu may be attributed to the underlying purple layer serving as darker background (Figs. 4, 8a), the other elements could be attributed to the earth pigment, as also evidenced by the ATR-FTIR spectra (ca. 3554, 3530, 1073, 968, 680 cm^{-1}; Table 3; Fig. 8c) and reflectance curve (Fig. 8d) [66,71].

Under the digital microscope, the pictorial surface is not uniform in colour, with yellow, white, green, and red grains in a matrix ranging from light to dark green (Fig. 8e). Green earth pigments generally have a low covering power. It is worth noting that the olive hue might be due to the presence of ferromagnesian compounds (such as celadonite) commonly found in earths derived from the alteration of volcanic rocks [84,85]. Considering the location of the site in the Vesuvius area, the possible use of locally-outcropping green earth pigments cannot be excluded [86].

Blue

The blue pigment was preserved on PAS 2 (Fig. 8e). It was characterised by blue crystals dispersed in a whitish matrix (DM in Fig. 8e) and XRF analysis revealed the presence of Cu, along with Ca and Fe (Table 3; Fig. 8b). ATR-FTIR spectra showed absorption bands at 1158, 1047, 1004, 792, 755, 663, 593, 517, 467 cm^{-1} (Table 3; Fig. 8c) and FORS curves were characterised by two absorption bands near 800 nm and 630 nm and reflectance maxima near 500 nm and 730 nm (Table 3; Fig. 8d). All these features are typical of Egyptian blue, a synthetic pigment containing a calcium and copper tetra-silicate, known in its natural mineralogical form as cuprorivaite ($CaCuSi_4O_{10}$) [87,88]. It was artificially synthetized by melting a sand containing quartz, feldspar, and carbonates with copper colouring compounds and alkaline flux, then allowing the mixture to slowly cool to form calcium and copper silicate crystals. Egyptian Blue was the first human-made pigment in history, largely used across the Mediterranean. Although it was first discovered in pharaonic contexts in Egypt of around the 3rd millennium BCE, the Romans quickly appreciated the unique qualities of this pigment and began reproducing it extensively in the Bay of Naples [38].

Yellow

Fragment PAS 1 (Fig. 9a,b) preserved the yellow pigment, although small yellow spots were also observed on the surface of sample PAS 4 (Fig. 4). XRF analyses revealed more intense peaks of Fe and Ca and Al, K and traces of Sr (Table 3; Fig. 9c). ATR-FTIR, instead, detected kaolinite ($Al_2Si_2O_5(OH)_4$), a clayey mineral with adsorption bands at ca. 3694, 3617, 1029, 912, 795, 531, 467, 426 cm^{-1} (Table 3; Fig. 9d). Although this latter is a constituent of the pigment, the main colouring compound is the iron hydroxide. RS showed the typical Raman shifts of goethite (FeO(OH)) at 568 and 385 cm^{-1} and FORS curve displayed the diagnostic absorption bands near 550, 660 and 930 nm (Table 3) [35]. This mineral, observed along with clay minerals, represents the main constituent of yellow ochre, an earth pigment largely used from the Palaeolithic [89].

4.2.3. Painting techniques

As already pointed out for the wall paintings from the pre-79 CE context, different painting techniques featured the wall painting from *villa*. Different pictorial layers overlapped the plasters (except for PAS 1) visible linear decorations or small spots details or overpainted surfaces as in PAS 4, where the green pictorial layer was spread on a purple background (Fig. 8a).

The microscopic observation illuminates the stratigraphy and the relation between *intonachino* and the painting layers, making the definition of the application technique quite clear. As in the samples from the *villa* of the previous building phase, in most of the cases of background colours the painting technique was the *mezzo-fresco*, as pigments are partially embedded into the underlying plaster layer, the thicknesses of the painting layer far exceed the grain size of the pigment, and some white portions intermixed with the pigment can be observed, probably due to calcite (Fig. 8a,e). An exception is the blue background of sample PAS 2. In fact, it presents a homogenously higher thickness (reaching 180 μm) and a clear contact with the underlying plaster.

Also here, the pigments applied on the background as decorations were painted by lime-based technique as a clear contact surface resulting in a clear discontinuity with the underlying layer has been observed (Fig. 8a,e).

5. Conclusions

The Roman context located in *Pollena Trocchia* has provided an ideal setting for investigating the use of pigments and painting technique in two consecutive chronological phases marked by the Vesuvius eruptions of 79 and 472 CE.

Decorated plasters elucidates that the ancient masters worked “layer by layer”, from the supports to the pictorial layer (Fig. 10). Intriguingly, the analyses have revealed a different technology in making supports and painting the walls.

Regarding the paintings, data have revealed that natural and synthetic pigments, either pure or mixed, were used to achieve the desired artistic effects. Red shades were made with different recipes and different pigments, from the red ochre in pure form or mixed with *minium,* to the cinnabar. Purple decorations were diachronically obtained by mixing Fe- and Pb-red pigments with Egyptian blue as well as the green shades, made by using green earths containing celadonite with Egyptian blue, in different proportion to obtain specific, more brilliant

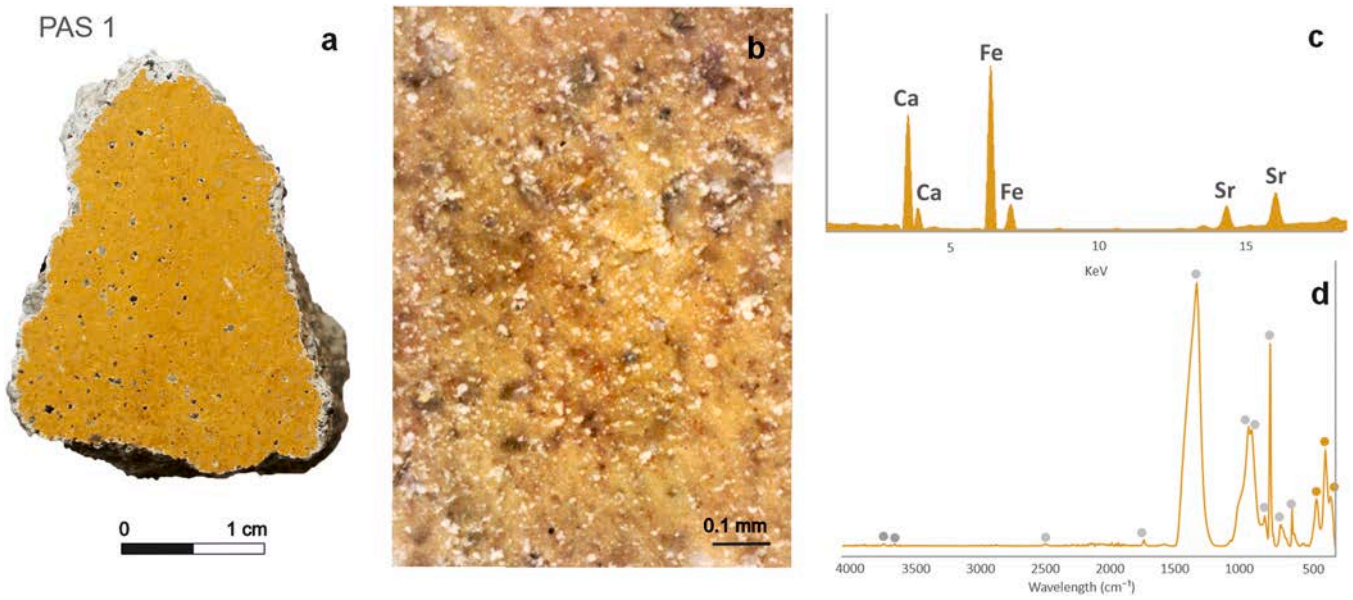

Fig. 9. Yellow paint on PAS 1 sample (a) observed by DM (b); spectroscopic results obtained by XRF (c) and ATR-FTIR (d) analyses.

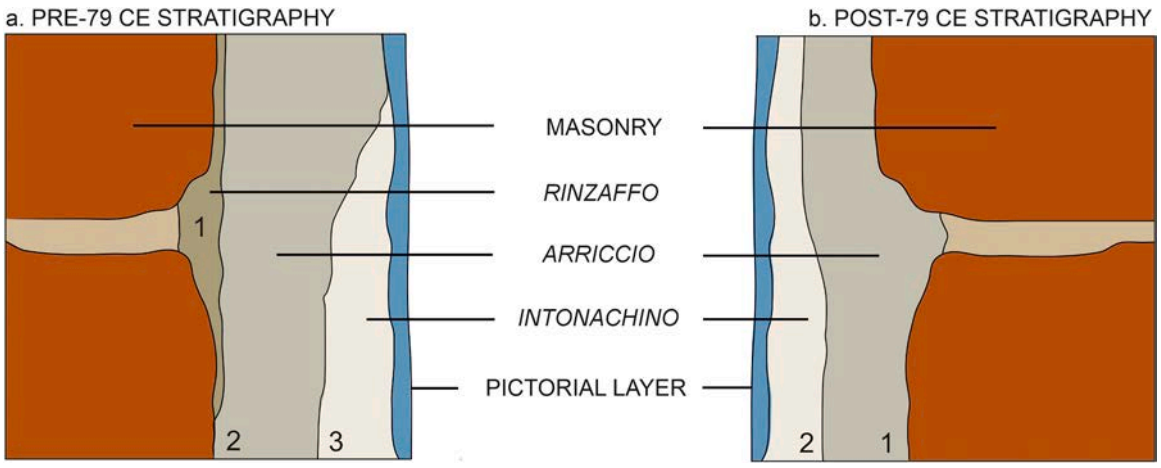

Fig. 10. Sketch sections of multi-layer stratigraphy of plasters consisting of three (a) or two layers (b) of plasters from the pre- and post-79 CE buildings (modified from [39]).

shade of green. Egyptian blue was also used as pure pigment for the blueish background, yellow ochre was used for yellow decorations, carbon black for the black ones. The main difference has been observed in the white pigments, which changed over time. In fact, calcite and/or dolomite were used to decorate background and white details in the pre-79 CE *villa*, whereas in the post-79 CE *villa* the use of aragonite has been attested, as also observed for other Roman context dated back to the same historical periods. Actually, it is well-documented the widespread use of aragonite as a specific white pigment after the Augustan period, which replaced the calcite and dolomite, largely used before.

Regarding the painting techniques, *mezzo-fresco* and lime-based techniques (using limewater or slaked lime suspension) were adopted for the backgrounds and for drawing details decorations. In one sample from the pre-79 CE *villa*, however, a thin glossy film above a pictorial decoration appears to be a compound of an organic nature, probably used as a coating for a highly unstable pigment (i.e., cinnabar).

Regarding the supports, a multi-layer technology has been observed for both buildings. However, samples from the *villa* built before the 79 CE eruption have generally showed three layers (Fig. 10a) below the pictorial layer. *Rinzaffo* and *arriccio* consisted in pozzolanic mortars whereas the *intonachino* in a *marmorino* layer, the latter proving of the wealth of the *villa*. The wall painting supports of the *villa* built after the 79 CE eruption, instead, consist of two layers of plasters (Fig. 10b), namely *arriccio* and *intonachino*, the former containing volcanic aggregate, the latter containing limestones with microfossils as aggregate, consistent with geological materials of calcareous nature readily available in the nearby landscape. However, the difference of the aggregates of the *intonachino* layers could be read as different raw material procurement. Instead of applying *intonachino* layer on some areas of the walls or ceiling, it was chosen to directly apply the pictorial layer on a plaster that closely resembles the composition of the *arriccio*.

The study contributes to the extensive research on wall painting in the Vesuvian area. The characterization of wall paintings leads us to reflect on the continuity of use of some pigments and mixtures not only within the same context but also across the Campania region, as evidenced by the comparison of pigments employed over time in this area [90]. This continuity is likewise observable in the modus operandi of the local workshops, which produce synthetic pigments but mostly use local raw materials [90]. The revealed multi-layer technology consisting of three layers agrees with those studied in the nearby contexts of *Pompeii*,

Herculaneum, *Stabiae* and Cuma [12,39,40,91]. Furthermore, the stratigraphy of the Villa of Papyri in *Herculaneum* has also evidenced the presence of only two layers [92]. In these instances as well, the numbering of plaster layers differ from the stratigraphy provided by the ancient authors [38,60] and it is evident that there is no fixed rule governing the art of building (Fig. 10). The different multi-layer technologies, often found within the same context, cannot be confined to a rigid formula. Moreover, in singular contexts, the variation in plaster layers could be linked to the specific location of the fragments on the original wall. It is worth noting that the studies carried out on the buried fragments only consider a section of the wall which may not fully represent the original stratigraphy. If the absence of scratch coat can be justified by poor conservation of the sample or by direct adhesion to the masonry, the lack of *intonachino,* as a fine carbonate-based layer, may be explained with a different location or function.

Nevertheless, reconstructing the multi-layer technology used in a broader context with a limited number of samples proves to be challenging.

A more comprehensive exploration of these technological choices becomes feasible when the archaeological contexts are exceptionally well-preserved, maintaining the wall paintings in their original spatial arrangement. In such instances, an extensive analysis campaign can be executed by non-destructive techniques performed in situ [93]. On the contrary, as in the case under consideration, the absence of painted plasters in-situ hinders the ability to make technological assessments in relation to their original location. The analysis of fragments coming from excavation materials, therefore, imposes a limit on the research. In such contexts, an expanded sampling strategy holds the potential to offer valuable insights into the methods employed into the ancient masters' "working steps", taking into account architectural and aesthetic considerations. Conversely, archaeometric studies carried out with fragments sourced from excavation materials entail a larger volume of material for analyses, a choice suitable for addressing archaeological and methodological questions related to dating [94].

The well-established chronological constraints of these plasters' fragments will be provided by mortar dating procedures on a selection of carbonate aggregate-free *arriccio* layers, further enriching the understanding of multiple construction phases of the studied archaeological context.

CRediT authorship contribution statement

Pagano Sabrina: Writing – review & editing, Writing – original draft, Visualization, Investigation, Formal analysis. **Germinario Chiara:** Writing – review & editing, Writing – original draft, Methodology, Investigation, Funding acquisition, Formal analysis, Conceptualization. **De Bonis Alberto:** Writing – review & editing, Investigation. **Mercurio Mariano:** Writing – review & editing, Investigation. **De Simone Girolamo Ferdinando:** Writing – review & editing, Project administration. **Piovesan Rebecca:** Writing – review & editing, Visualization. **d'Aniello Francesca:** Writing – review & editing, Investigation. **Grifa Celestino:** Writing – review & editing, Supervision, Methodology, Funding acquisition, Conceptualization.

Declaration of Competing Interest

The authors declare that they have no known competing financial interests or personal relationships that could have appeared to influence the work reported in this paper.

Data Availability

Data will be made available on request.

Acknowledgements

The authors would like to thank the two anonymous reviewers for their valuable suggestions, giving us the opportunity to improve the paper. This work was supported by grants of the Department of Sciences and Technologies of University of Sannio (FRA Grifa and FRA Germinario).

Appendix A. Supporting information

Supplementary data associated with this article can be found in the online version at doi:10.1016/j.conbuildmat.2023.134441.

References

[1] E.M. Moormann, Roman wall painting, Encycl. Glob. Archaeol. (2018) 1–22, https://doi.org/10.1007/978-3-319-51726-1_3405-1.
[2] M.F. Alberghina, C. Germinario, G. Bartolozzi, S. Bracci, C. Grifa, F. Izzo, M.F. La Russa, D. Magrini, E. Massa, M. Mercurio, V.M. Nardo, M.E. Oddo, S.M. Pagnotta, A. Pelagotti, R.C. Ponterio, P. Ricci, N. Rovella, S.A. Ruffolo, S. Schiavone, A. Spagnuolo, C. Vetromile, G. Zuchtriegel, C. Lubritto, Non-invasive characterization of the pigment's palette used on the painted tomb slabs at Paestum archaeological site, : IOP Conf. Ser. Mater. Sci. Eng. (2020), 012002, https://doi.org/10.1088/1757-899X/949/1/012002.
[3] E. Gliozzo, A. Pizzo, M.F. La Russa, Mortars, plasters and pigments—research questions and sampling criteria, Archaeol. Anthr. Sci. 13 (2021), https://doi.org/10.1007/s12520-021-01393-2.
[4] M. Aceto, Pigments—the palette of organic colourants in wall paintings, Archaeol. Anthr. Sci. 13 (2021), https://doi.org/10.1007/s12520-021-01392-3.
[5] G.A. Mazzocchin, F. Agnoli, S. Mazzocchin, I. Colpo, Analysis of pigments from Roman wall paintings found in Vicenza, Talanta 61 (2003) 565–572, https://doi.org/10.1016/S0039-9140(03)00323-0.
[6] R. Radpour, C. Fischer, I. Kakoulli, New insight into hellenistic and roman cypriot wall paintings: an exploration of artists' materials, production technology, and technical style, Arts 8 (2019) 74, https://doi.org/10.3390/arts8020074.
[7] C. Balandier, C. Joliot, M. Ménager, F. Vouve, C. Vieillescazes, Chemical analyses of Roman wall paintings recently found in Paphos, Cyprus: the complementarity of archaeological and chemical studies, J. Archaeol. Sci. Rep. 14 (2017) 332–339, https://doi.org/10.1016/j.jasrep.2017.06.016.
[8] J. Cuní, What do we know of Roman wall painting technique? Potential confounding factors in ancient paint media analysis, Herit. Sci. 4 (2016) 1–13, https://doi.org/10.1186/s40494-016-0111-4.
[9] F. Casadio, I. Giangualano, F. Pique, Organic materials in wall paintings: the historical and analytical literature, Stud. Conserv. 49 (2004) 63–80, https://doi.org/10.1179/sic.2004.49.Supplement-1.63.
[10] L. Regazzoni, G. Cavallo, D. Biondelli, J. Gilardi, Microscopic analysis of wall painting techniques: laboratory replicas and romanesque case studies in Southern Switzerland, Stud. Conserv. 63 (2018) 326–341, https://doi.org/10.1080/00393630.2017.1422891.
[11] M. Salvadori, C. Sbrolli, Wall paintings through the ages: the roman period—Republic and early Empire, Archaeol. Anthr. Sci. 13 (2021), 187, https://doi.org/10.1007/s12520-021-01411-3.
[12] R. Piovesan, C. Mazzoli, L. Maritan, Production recipes of mortar-based materials from ancient Pompeii by quantitative image analysis approach: the microstratigraphy of plasters in the Temple of Venus, J. Cult. Herit. 59 (2023) 57–68, https://doi.org/10.1016/j.culher.2022.11.002.
[13] M. Secco, L. Rainer, K. Graves, A. Heginbotham, G. Artioli, F. Piqué, I. Angelini, Ochre-based pigments in the tablinum of the house of the bicentenary (Herculaneum, Italy) between decorative technology and natural disasters, Minerals 11 (1) (2021) 30, https://doi.org/10.3390/min11010067.
[14] L. Birolo, A. Tomeo, M. Trifuoggi, F. Auriemma, L. Paduano, A. Amoresano, R. Vinciguerra, C. De Rosa, L. Ferrara, A. Giarra, A. Luchini, C. De Maio, G. Greco, A. Vergara, A hypothesis on different technological solutions for outdoor and indoor Roman wall paintings, Archaeol. Anthr. Sci. 9 (2017) 591–602, https://doi.org/10.1007/s12520-016-0408-y.
[15] A. Casoli, S. Santoro, Organic materials in the wall paintings in Pompei: a case study of Insula del Centenario, Chem. Cent. J. 6 (2012), 107, https://doi.org/10.1186/1752-153X-6-107.
[16] A. Mau, Geschichte der decorativen Wandmalerei in Pompeji, Berlino, Germany, 1882.
[17] M.F. Alberghina, C. Germinario, G. Bartolozzi, S. Bracci, C. Grifa, F. Izzo, M.F. La Russa, D. Magrini, E. Massa, M. Mercurio, V.M. Nardo, M.E. Oddo, S.M. Pagnotta, A. Pelagotti, R.C. Ponterio, P. Ricci, N. Rovella, S.A. Ruffolo, S. Schiavone, A. Spagnuolo, C. Vetromile, G. Zuchtriegel, C. Lubritto, The Tomb of the Diver and the frescoed tombs in Paestum (southern Italy): New insights from a comparative archaeometric study, PLoS One 15 (2020), e0232375.
[18] D. Miriello, A. Bloise, G.M. Crisci, R. De Luca, B. De Nigris, A. Martellone, M. Osanna, R. Pace, A. Pecci, N. Ruggieri, New compositional data on ancient mortars and plasters from Pompeii (Campania – Southern Italy): Archaeometric results and considerations about their time evolution, Mater. Charact. 146 (2018) 189–203, https://doi.org/10.1016/j.matchar.2018.09.046.

[19] R. De Luca, D. Miriello, A. Pecci, S. Domínguez-Bella, D. Bernal-Casasola, D. Cottica, A. Bloise, G.M. Crisci, Archaeometric Study of Mortars from the Garum Shop at Pompeii, Campania, Italy, Geoarchaeology 30 (2015) 330–351, https://doi.org/10.1002/gea.21515.

[20] D. Miriello, D. Barca, A. Bloise, A. Ciarallo, G.M. Crisci, T. De Rose, C. Gattuso, F. Gazineo, M.F. La Russa, Characterisation of archaeological mortars from Pompeii (Campania, Italy) and identification of construction phases by compositional data analysis, J. Archaeol. Sci. 37 (2010) 2207–2223.

[21] S. Pérez-Diez, F. Caruso, E.F. Nardini, M. Stollenwerk, M. Maguregui, Secco painting technique revealed in non-restored Pompeian murals by analytical and imaging techniques, Microchem. J. 194 (2023), 109365, https://doi.org/10.1016/j.microc.2023.109365.

[22] R. Piovesan, R. Siddall, C. Mazzoli, L. Nodari, The Temple of Venus (Pompeii): A study of the pigments and painting techniques, J. Archaeol. Sci. 38 (2011) 2633–2643, https://doi.org/10.1016/j.jas.2011.05.021.

[23] C.S. Martucci, G. Boemio, G. Trojsi, G.F.De Simone, Pollena Trocchia (NA), località Masseria De Carolis, L'analisi dei Reper. per la Ricostr. Del. Contest Econ. e Soc. della Villa Romana, Amoenitas II (2012) 87–117.

[24] G.F. De Simone, R.T. Macfarlane, Apolline project vol.1: Studies on Vesuvius' north slope and the Bay of Naples, Università Suor Orsola Benincasa and Brigham Young University, 2009.

[25] C. Germinario, G. Cultrone, A. De Bonis, G.F. De Simone, M. Gorrasi, F. Izzo, A. Langella, C.S. Martucci, M. Mercurio, V. Morra, C.R. Vyhnal, C. Grifa, Production technology of late Roman decorated tableware from the Vesuvius environs: Evidence from Pollena Trocchia (Campania region, Italy), Geoarchaeology 36 (2021) 34–53, https://doi.org/10.1002/gea.21819.

[26] E. De Carolis, G. Soricelli, Il sito di via Lepanto a Pompei: brevi note sul Tardoantico in area vesuviana, in: Volpe, Turchiano (Eds.), Paesaggi e Insediamenti Rurali in Italia Meridionale Fra Tardoantico e Altomedioevo, 2005: pp. 513–527.

[27] G. Soricelli, Divisioni agrarie romane e occupazione del territorio nella piana nocerino-sarnese, in: G. Franciosi (Ed.), Ager Campanus. La Storia Dell'ager Campanus, i Problemi Della Limitatio e Sua Lettura Attuale, Jovene Editore, Naples, Italy, 2002, pp. 123–129.

[28] G.F. De Simone, A. Perrotta, C. Scarpati, A. De Simone, R.T. Macfarlane, Episodi vulcanici e vulcanoclastici (V-XVII secolo) che hanno sepolto un edificio romano a Pollena Trocchia (Italia), Alp. Mediterr. Quat. 22 (2009) 53–60.

[29] G. De Simone, V. Castaldo, S. Sannino, Four pottery assemblages buried by late antique eruptions of Vesuvius, 45 (2018) 299–309.

[30] L. Bonizzoni, S. Caglio, A. Galli, C. Germinario, F. Izzo, D. Magrini, Identifying Original and Restoration Materials through Spectroscopic Analyses on Saturnino Gatti Mural Paintings: How Far a Noninvasive Approach Can Go, Appl. Sci. 13 (2023), https://doi.org/10.3390/app13116638.

[31] G. Montana, R. Giarrusso, R. D'Amico, B. Di Natale, M.A. Vizzini, V. Ilardi, A. Mulone, L. Randazzo, C.V. Bordenca, Multi-analytical study of the medieval wall paintings from the rupestrian church Grotta del Crocifisso at Lentini (eastern Sicily): new evidence of the use of woad (Isatis tinctoria), Archaeol. Anthr. Sci. 14 (2022), 183, https://doi.org/10.1007/s12520-022-01656-6.

[32] S. Bracci, E. Cantisani, C. Conti, D. Magrini, V. Silvia, P. Tomassini, M. Marano, Enriching the knowledge of Ostia antica painted fragments: A multi-methodological approach, Spectrochim. Acta A Mol. Biomol. Spectrosc. 265 (2022), 120260, https://doi.org/10.1016/j.saa.2021.120260.

[33] M.L. Amadori, I. Costantini, J.M. Madariaga Mota, L. Valentini, F. Ferrucci, V. Mengacci, M. Camaiti, Calcium antimonate: A new discovery in colour palette of Paestum wall paintings, Microchem. J. 168 (2021), 106401, https://doi.org/10.1016/j.microc.2021.106401.

[34] V. Guglielmi, M. Andreoli, V. Comite, A. Baroni, P. Fermo, The combined use of SEM-EDX, Raman, ATR-FTIR and visible reflectance techniques for the characterisation of Roman wall painting pigments from Monte d'Oro area (Rome): an insight into red, yellow and pink shades, Environ. Sci. Pollut. Res. 29 (2022) 29419–29437, https://doi.org/10.1007/s11356-021-15085-w.

[35] E. Cheilakou, M. Troullinos, M. Koui, Identification of pigments on Byzantine wall paintings from Crete (14th century AD) using non-invasive Fiber Optics Diffuse Reflectance Spectroscopy (FORS), J. Archaeol. Sci. 41 (2014) 541–555, https://doi.org/10.1016/j.jas.2013.09.020.

[36] I. Fikri, M. El Amraoui, M. Haddad, A.S. Ettahiri, C. Falguères, L. Bellot-Gurlet, T. Lamhasni, S. Ait Lyazidi, L. Bejjit, Raman and ATR-FTIR analyses of medieval wall paintings from al-Qarawiyyin in Fez (Morocco), Spectrochim. Acta A Mol. Biomol. Spectrosc. 280 (2022), 121557, https://doi.org/10.1016/j.saa.2022.121557.

[37] R.D. Terry, G.V. ChilingarSummary of "Concerning some additional aids in studying sedimentary formations" by M.S. Shvetsov, J Sediment Petrol. 25 (1955) 229–234. https://doi.org/10.1306/74D70466–2B21–11D7–8648000102C1865D.

[38] N.H. Morgan, Vitruvius. The ten books on architecture, in: Vitruvius. The ten books on architecture, Dover Publications, New York, 1960, p. 331.

[39] F. Izzo, A. Arizzi, P. Cappelletti, G. Cultrone, A. De Bonis, C. Germinario, S. F. Graziano, C. Grifa, V. Guarino, M. Mercurio, V. Morra, A. Langella, The art of building in the Roman period (89 B.C. - 79 A.D.): Mortars, plasters and mosaic floors from ancient Stabiae (Naples, Italy), Constr. Build. Mater. 117 (2016) 129–143, https://doi.org/10.1016/j.conbuildmat.2016.04.101.

[40] C. Germinario, S. Pagano, M. Mercurio, F. Izzo, A. De Bonis, V. Morra, P. Munzi, M. Leone, E. Conca, C. Grifa, Roman technological expertise in the construction of perpetual buildings: new insights into the wall paintings of a banquet scene from a tomb in Cumae (southern Italy), Archaeol. Anthr. Sci. 14 (2022), https://doi.org/10.1007/s12520-022-01651-x.

[41] S. Pagano, C. Germinario, M.F. Alberghina, M. Covolan, M. Mercurio, D. Musmeci, R. Piovesan, A. Santoriello, S. Schiavone, C. Grifa, Multilayer Technology of Decorated Plasters from the domus of Marcus Vipsanus Primigenius at Abellinum (Campania Region, Southern Italy): An Analytical Approach, Minerals 12 (2022), https://doi.org/10.3390/min12121487.

[42] L. Maritan, G. Ganzarolli, F. Antonelli, M. Rigo, A. Kapatza, K. Bajnok, C. Coletti, C. Mazzoli, L. Lazzarini, P. Vedovetto, A. Chavarría Arnau, What kind of calcite? Disclosing the origin of sparry calcite temper in ancient ceramics, J. Archaeol. Sci. 129 (2021), 105358, https://doi.org/10.1016/j.jas.2021.105358.

[43] R. Piovesan, E. Curti, C. Grifa, L. Maritan, C. Mazzoli, Petrographic & Microstratigraphic Analysis of Mortar-Based Building Materials From the Temple of Venus, Pompeii, in: P.S. Quinn (Ed.), Interpreting Silent Artefacts: Petrographic Approaches to Archaeological Ceramics, Archeopress, 2009, pp. 65–80.

[44] S. Dilaria, M. Secco, M. Rubinich, J. Bonetto, D. Miriello, D. Barca, G. Artioli, High-performing mortar-based materials from the late imperial baths of Aquileia: An outstanding example of Roman building tradition in Northern Italy, Geoarchaeology 37 (2022) 637–657, https://doi.org/10.1002/gea.21908.

[45] C.M. Belfiore, G.V. Fichera, M.F. La Russa, A. Pezzino, S.A. Ruffolo, G. Galli, D. Barca, A Multidisciplinary Approach for the Archaeometric Study of Pozzolanic Aggregate in Roman Mortars: The Case of Villa dei Quintili (Rome, Italy), Archaeometry 57 (2015) 269–296, https://doi.org/10.1111/arcm.12085.

[46] F. Izzo, C. Grifa, C. Germinario, M. Mercurio, A. De Bonis, L. Tomay, A. Langella, Production technology of mortar-based building materials from the Arch of Trajan and the Roman Theatre in Benevento, Italy, Eur. Phys. J. 133 (2018), 363, https://doi.org/10.1140/epjp/i2018-12229-1.

[47] G.A. Mazzocchin, E.F. Orsega, P. Baraldi, P. Zannini, Aragonite in Roman wall paintings of the VIII Regio, Aemilia, and X Regio, Venetia et Histria, (2006) 377–387.

[48] F. Izzo, C. Germinario, C. Grifa, A. Langella, M. Mercurio, External reflectance FTIR dataset (4000–400 cm−1) for the identification of relevant mineralogical phases forming Cultural Heritage materials, Infrared Phys. Technol. 106 (2020), 103266, https://doi.org/10.1016/j.infrared.2020.103266.

[49] J. Katarzyna, Stanienda-Pilecki, The Importance of Fourier-Transform Infrared Spectroscopy in the Identification of Carbonate Phases Differentiated in Magnesium Content, Spectroscopy 34 (2019) 32–42.

[50] L. Borromeo, N. Egeland, M. Wetrhus Minde, U. Zimmermann, S. Andò, M. V. Madland, R.I. Korsnes, Quick, Easy, and Economic Mineralogical Studies of Flooded Chalk for EOR Experiments Using Raman Spectroscopy, Minerals 8 (2018), https://doi.org/10.3390/min8060221.

[51] R. Siddall, Not a day without a line drawn: Pigments and painting techniques of Roman Artists, Focus Mag.: Proc. R. Microsc. Soc. 2 (2006) 18–23, https://doi.org/10.22443/RMS.INF.1.4.

[52] E.P. Tomasini, E.B. Halac, M. Reinoso, E.J. Di Liscia, M.S. Maier, Micro-Raman spectroscopy of carbon-based black pigments, J. Raman Spectrosc. 43 (2012) 1671–1675.

[53] A. Coccato, J. Jehlicka, L. Moens, P. Vandenabeele, Raman spectroscopy for the investigation of carbon-based black pigments, J. Raman Spectrosc. 46 (2015) 1003–1015, https://doi.org/10.1002/jrs.4715.

[54] M. Menu, L'analyse de l'art préhistorique, Anthropologie 113 (2009) 547–558, https://doi.org/10.1016/j.anthro.2009.09.011.

[55] A. Bonneau, D.G. Pearce, A.M. Pollard, A multi-technique characterization and provenance study of the pigments used in San rock art, South Africa, J. Archaeol. Sci. 39 (2012) 287–294, https://doi.org/10.1016/j.jas.2011.09.011.

[56] M. Bouchard, D.C. Smith, Catalogue of 45 reference Raman spectra of minerals concerning research in art history or archaeology, especially on corroded metals and coloured glass, Spectrochim. Acta A Mol. Biomol. Spectrosc. 59 (2003) 2247–2266, https://doi.org/10.1016/S1386-1425(03)00069-6.

[57] S. Augusti, Colori pompeiani, Rome, 1967.

[58] M. Cotte, J. Susini, N. Metrich, A. Moscato, C. Gratziu, A. Bertagnini, M. Pagano, Blackening of Pompeian cinnabar paintings: X-ray microspectroscopy analysis, Anal. Chem. 78 (2006) 7484–7492.

[59] M.K. Neiman, M. Balonis, I. Kakoulli, Cinnabar alteration in archaeological wall paintings: an experimental and theoretical approach, Appl. Phys. A 121 (2015) 915–938.

[60] H. Rackham, Pliny the Elder. Natural History in Ten Volumes, Loeb Classical Library, Cambridge, 1968.

[61] R. Nöller, Cinnabar reviewed: Characterization of the red pigment and its reactions, Stud. Conserv. 60 (2015) 79–87, https://doi.org/10.1179/2047058413Y.0000000089.

[62] S. Pérez-Diez, A. Pitarch Martí, A. Giakoumaki, N. Prieto-Taboada, S. Fdez-Ortiz de Vallejuelo, A. Martellone, B. De Nigris, M. Osanna, J.M. Madariaga, M. Maguregui, When Red Turns Black: Influence of the 79 AD Volcanic Eruption and Burial Environment on the Blackening/Darkening of Pompeian Cinnabar, Anal. Chem. 93 (2021) 15870–15877, https://doi.org/10.1021/acs.analchem.1c02420.

[63] M. Aceto, A. Agostino, G. Fenoglio, A. Idone, M. Gulmini, M. Picollo, P. Ricciardi, J.K. Delaney, Characterisation of colourants on illuminated manuscripts by portable fibre optic UV–visible-NIR reflectance spectrophotometry, Anal. Methods 6 (2014) 1488–1500, https://doi.org/10.1039/c3ay41904e.

[64] B. Fonseca, C. Schmidt Patterson, M. Ganio, D. MacLennan, K. Trentelman, Seeing red: towards an improved protocol for the identification of madder- and cochineal-based pigments by fiber optics reflectance spectroscopy (FORS), Herit. Sci. 7 (2019), 92, https://doi.org/10.1186/s40494-019-0335-1.

[65] K. Helwig, The characterisation of iron earth pigments using infrared spectroscopy, in: Victoria&Albert Museum (Ed.), Proceedings of the Second Infrared and Raman User's Group (IRUG 2) Conference, 12–13 September 1995, Victoria&Albert Museum, London, UK, 1995: pp. 83–92.

[66] A. Cosentino, FORS Spectral Database of Historical Pigments in Different Binders, E-Conserv. J. (2014) 54–65, https://doi.org/10.18236/econs2.201410.
[67] L.F.C. de Oliveira, H.G.M. Edwards, R.L. Frost, J.T. Kloprogge, P.S. Middleton, Caput mortuum: Spectroscopic and structural studies of an ancient pigment, Analyst 127 (2002) 536–541, https://doi.org/10.1039/b111473p.
[68] R.M. Ion, M.G. Barbu, A. Gonciar, G. Vasilievici, A.I. Gheboianu, S. Slamnoiu-Teodorescu, M.E. David, L. Iancu, R.M. Grigorescu, A Multi-Analytical Investigation of Roman Frescoes from Rapoltu Mare (Romania), Coatings 12 (2022), https://doi.org/10.3390/coatings12040530.
[69] S.E. Jorge-Villar, H.G.M. Edwards, Green and blue pigments in Roman wall paintings: A challenge for Raman spectroscopy, J. Raman Spectrosc. 52 (2021) 2190–2203, https://doi.org/10.1002/jrs.6118.
[70] C. Germinario, F. Izzo, M. Mercurio, A. Langella, D. Sali, I. Kakoulli, A. De Bonis, C. Grifa, Multi-analytical and non-invasive characterization of the polychromy of important archaeological wall paintings at the Domus of Octavius Quartio in Pompeii, Eur. Phys. J. 133 (2018), 359, https://doi.org/10.1140/epjp/i2018-12224-6.
[71] I. Aliatis, D. Bersani, E. Campani, A. Casoli, P.P. Lottici, S. Mantovan, I.G. Marino, F. Ospitali, Green pigments of the Pompeian artists' palette, Spectrochim. Acta A Mol. Biomol. Spectrosc. 73 (2009) 532–538, https://doi.org/10.1016/j.saa.2008.11.009.
[72] F. Ospitali, D. Bersani, G. Di Lonardo, P.P. Lottici, 'Green earths': vibrational and elemental characterization of glauconites, celadonites and historical pigments, J. Raman Spectrosc. Spectrosc. 39 (2008) 1066–1073.
[73] L.M. Moretto, E.F. Orsega, G.A. Mazzocchin, Spectroscopic methods for the analysis of celadonite and glauconite in Roman green wall paintings, J. Cult. Herit. 12 (2011) 384–391, https://doi.org/10.1016/j.culher.2011.04.003.
[74] A. Fanost, A. Gimat, L. de Viguerie, P. Martinetto, A.C. Giot, M. Clémancey, G. Blondin, F. Gaslain, H. Glanville, P. Walter, G. Mériguet, A.L. Rollet, M. Jaber, Revisiting the identification of commercial and historical green earth pigments, Colloids Surf. A Physicochem Eng. Asp. 584 (2020), 124035, https://doi.org/10.1016/j.colsurfa.2019.124035.
[75] Shigeru Tsuji, The Origins of buon fresco, Z. Kunst. 46 (1983) 215–222.
[76] R. Piovesan, C. Mazzoli, L. Maritan, P. Cornale, Fresco and lime-paint: An experimental study and objective criteria for distinguishing between these painting techniques, Archaeometry 54 (2012) 723–736, https://doi.org/10.1111/j.1475-4754.2011.00647.x.
[77] O. Cristini, C. Kinowski, S. Turrell, A detailed micro-Raman spectroscopic study of wall paintings of the periodAD 100-200: Effect of atmospheric conditions on the alteration of samples, J. Raman Spectrosc. 41 (2010) 1410–1417, https://doi.org/10.1002/jrs.2656.
[78] E.J. Cerrato, D. Cosano, D. Esquivel, C. Jiménez-Sanchidrián, J.R. Ruiz, Spectroscopic analysis of pigments in a wall painting from a high Roman Empire building in Córdoba (Spain) and identification of the application technique, Microchem. J. 168 (2021), 106444, https://doi.org/10.1016/j.microc.2021.106444.
[79] A. Kriznar, J. Želinská, Materials and techniques of selected mural paintings on the "gothic road" around 1400 (Slovakia), Heritage 4 (2021) 4105–4125, https://doi.org/10.3390/heritage4040226.
[80] S. Gunasekaran, G. Anbalagan, S. Pandi, Raman and infrared spectra of carbonates of calcite structure, J. Raman Spectrosc. 37 (2006) 892–899.
[81] C. Paolini, M. Faldi, Glossario delle tecniche artistiche e del restauro, eds. Palaz, Firenze, Italy, 2000.
[82] G.A. Mazzocchin, A. Vianello, S. Minghelli, D. Rudello, Analysis of roman wall paintings from the thermae of "Iulia Concordia, Archaeometry 52 (2010) 644–655, https://doi.org/10.1111/j.1475-4754.2009.00501.x.
[83] G.A. Mazzocchin, M. Del Favero, G. Tasca, Analysis of pigments from roman wall paintings found in the "agro centuriato" of Julia Concordia (ITALY), Ann. Chim. 97 (2007) 905–913, https://doi.org/10.1002/adic.200790075.
[84] N. Eastaugh, V. Walsh, T. Chaplin, R. Siddall, Pigment Compendium: A Dictionary and Optical Microscopy of Historic Pigments, Butterworth-Heinemann, London, 2008.
[85] G. Giachi, E. De Carolis, P. Pallecchi, Raw materials in pompeian paintings: Characterization of some colors from the archaeological site, Mater. Manuf. Process. 24 (2009) 1015–1022, https://doi.org/10.1080/10426910902982631.
[86] M. Russo, I. Campostrini, Elenco delle specie minerali del "Somma-Vesuvio,", Misc. INGV 65 (2021) 1–36, https://doi.org/10.13127/misc/65.
[87] C. Grifa, L. Cavassa, A. De Bonis, C. Germinario, V. Guarino, F. Izzo, I. Kakoulli, A. Langella, M. Mercurio, V. Morra, I. Lloyd, Beyond Vitruvius: New Insight in the Technology of Egyptian Blue and Green Frits, J. Am. Ceram. Soc. 99 (2016) 3467–3475, https://doi.org/10.1111/jace.14370.
[88] H. Berke, The invention of blue and purple pigments in ancient times, Chem. Soc. Rev. 36 (2007) 15–30, https://doi.org/10.1039/B606268G.
[89] J.L. Mortimore, L.-J.R. Marshall, M.J. Almond, P. Hollins, W. Matthews, Analysis of red and yellow ochre samples from Clearwell Caves and Catalhoyok by vibrational spectroscopy and other techniques, Spectrochim. Acta A Mol. Biomol. Spectrosc. 60 (2004) 1179–1188, https://doi.org/10.1016/j.saa.2003.08.002.
[90] S. Pagano, C. Germinario, I. Di Santi, M. Mercurio, C. Grifa, Pigments through the ages: examples from archaeological contexts of Campania region (southern Italy), in: IMEKO TC4 International Conference on Metrology for Archaeology and Cultural Heritage, 2022: pp. 84–89. https://doi.org/10.21014/tc4-ARC-2022.017.
[91] G. Leone, A. De Vita, A. Magnani, C. Rossi, Characterization of archaeological mortars from Herculaneum, Thermochim. Acta 624 (2016) 86–94, https://doi.org/10.1016/j.tca.2015.12.003.
[92] M.L. Amadori, S. Barcelli, G. Poldi, F. Ferrucci, A. Andreotti, P. Baraldi, M. P. Colombini, Invasive and non-invasive analyses for knowledge and conservation of Roman wall paintings of the Villa of the Papyri in Herculaneum, Microchem. J. 118 (2014) 183–192, https://doi.org/10.1016/j.microc.2014.08.016.
[93] P. Arjonilla, A. Domínguez-Vidal, R. Rubio Domene, E. Correa Gómez, M.J. de la Torre-López, M.J. Ayora-Cañada, Characterization of wall paintings of the harem court in the alhambra monumental ensemble: advantages and limitations of in situ analysis, Molecules 27 (2022) 1490, https://doi.org/10.3390/molecules27051490.
[94] F. Marzaioli, S. Nonni, I. Passariello, M. Capano, P. Ricci, C. Lubritto, N. De Cesare, G. Eramo, J.A. Quirós Castillo, F. Terrasi, Accelerator mass spectrometry 14C dating of lime mortars: Methodological aspects and field study applications at CIRCE (Italy), Nucl. Instrum. Methods Phys. Res B 294 (2013) 246–251, https://doi.org/10.1016/j.nimb.2012.09.006.